

MIT Open Access Articles

The GMOX science case: resolving galaxies through cosmic time

The MIT Faculty has made this article openly available. **Please share** how this access benefits you. Your story matters.

Citation: Gennaro, Mario, et al. "The GMOX Science Case: Resolving Galaxies through Cosmic Time." Proceedings Volume 9908, Ground-based and Airborne Instrumentation for Astronomy VI, 25 June - 1 July, 2016, Edinburgh, United Kingdom, edited by Christopher J. Evans et al., 2016, SPIE, p. 990849. © 2016 SPIE

As Published: <http://dx.doi.org/10.1117/12.2232101>

Publisher: SPIE

Persistent URL: <http://hdl.handle.net/1721.1/116440>

Version: Final published version: final published article, as it appeared in a journal, conference proceedings, or other formally published context

Terms of Use: Article is made available in accordance with the publisher's policy and may be subject to US copyright law. Please refer to the publisher's site for terms of use.



PROCEEDINGS OF SPIE

[SPIDigitalLibrary.org/conference-proceedings-of-spie](https://spiedigitallibrary.org/conference-proceedings-of-spie)

The GMOX science case: resolving galaxies through cosmic time

Mario Gennaro, Massimo Robberto, Timothy Heckman, Stephen A. Smee, Robert Barkhouser, et al.

Mario Gennaro, Massimo Robberto, Timothy Heckman, Stephen A. Smee, Robert Barkhouser, Zoran Ninkov, Angela Adamo, George Becker, Andrea Bellini, Luciana Bianchi, Arjan Bik, Rongmon Bordoloi, Annalisa Calamida, Daniela Calzetti, Gisella De Rosa, Susana Deustua, Jason Kalirai, Jennifer Lotz, John MacKenty, Carlo Felice Manara, Margaret Meixner, Camilla Pacifici, Elena Sabbi, Kailash Sahu, Jason Tumlinson, "The GMOX science case: resolving galaxies through cosmic time," Proc. SPIE 9908, Ground-based and Airborne Instrumentation for Astronomy VI, 990849 (30 November 2016); doi: 10.1117/12.2232101

SPIE.

Event: SPIE Astronomical Telescopes + Instrumentation, 2016, Edinburgh, United Kingdom

The GMOX science case: resolving galaxies through cosmic time

Mario Gennaro^a, Massimo Robberto^{a,b}, Timothy Heckman^b, Stephen A. Smee^b,
Robert Barkhouser^b, Zoran Ninkov^c, Angela Adamo^d, George Becker^e, Andrea Bellini^a,
Luciana Bianchi^b, Arjan Bik^d, Rongmon Bordoloi^f, Annalisa Calamida^g, Daniela Calzetti^h,
Gisella De Rosa^a, Susana Deustua^a, Jason Kalirai^a, Jennifer Lotz^a, John MacKenty^a,
Carlo Felice Manaraⁱ, Margaret Meixner^a, Camilla Pacifici^j, Elena Sabbi^a, Kailash Sahu^a, and
Jason Tumilson^a

^aSpace Telescope Science Institute, 3700 San Martin Drive, Baltimore, MD 21218, USA

^bJohns Hopkins University, Department of Physics and Astronomy, 3701 San Martin Drive,
Baltimore, MD 21218, USA

^cRochester Institute of Technology, Center for Imaging Science, 54 Lomb Memorial Drive,
Rochester, NY 14623, USA

^dDepartment of Astronomy, Oskar Klein Centre, Stockholm University, SE-10691 Stockholm,
Sweden

^eUniversity of California Riverside, Department of Physics & Astronomy, Riverside, CA 92507,
USA

^fMassachusetts Institute of Technology, 77 Massachusetts Ave, Cambridge, MA 02139, USA

^gNational Optical Astronomy Observatory, 950 N Cherry Ave, Tucson, AZ 85719, USA

^hUniversity of Massachusetts Amherst, Amherst, MA 01003, USA

ⁱESA/ESTEC, Keplerlaan 1, 2201 AZ Noordwijk, Netherlands

^jGoddard Space Flight Center, 8800 Greenbelt Rd, Greenbelt, MD 20771

ABSTRACT

We present the key scientific questions that can be addressed by GMOX, a Multi-Object Spectrograph selected for feasibility study as a 4th generation instrument for the Gemini telescopes. Using commercial digital micro-mirror devices (DMDs) as slit selection mechanisms, GMOX can observe hundred of sources at $R \sim 5000$ between the U and K band simultaneously. Exploiting the narrow PSF delivered by the Gemini South GeMS MCAO module, GMOX can synthesize slits as small as 40mas reaching extremely faint magnitude limits, and thus enabling a plethora of applications and innovative science. Our main scientific driver in developing GMOX has been Resolving galaxies through cosmic time: GMOX 40mas slit (at GeMS) corresponds to 300 pc at $z \sim 1.5$, where the angular diameter distance reaches its maximum, and therefore to even smaller linear scales at any other redshift. This means tha GMOX can take spectra of regions smaller than 300 pc in the whole observable Universe, allowing to probe the growth and evolution of galaxies with unprecedented detail. GMOXs multi-object capability and high angular resolution enable efficient studies of crowded fields, such as globular clusters, the Milky Way bulge, the Magellanic Clouds, Local Group galaxies and galaxy clusters. The wide-band simultaneous coverage and the very fast slit configuration mechanisms also make GMOX ideal for followup of LSST transients.

Keywords: DMD, Spectrograph, Multi-Object, Adaptive Optics, Near Infrared, Camera, Wide-Band

Further author information: (Send correspondence to M.G.)

E-mail: gennaro@stsci.edu, Telephone: +1 410 338 4825

1. INTRODUCTION

The Gemini Multi-Object eXtra-wide-band spectrograph (GMOX) is an advanced concept for an instrument designed to be installed at the Gemini observatory. The development of GMOX has been prompted by a solicitation by the Gemini observatory, who is seeking to build their third instrument of the fourth generation (Gen4#3). The Gen4#3 instrument is envisioned by Gemini as a true *workhorse*: an instrument of high versatility and efficiency. Our proposed GMOX is a highly configurable multi-object spectrograph, where the slit selection mechanism is an array of Digital Micromirror Devices. Each micromirror, depending on the configuration, can see an area on the sky as small as 40mas, thus exploiting the adaptive optics systems of Gemini (either ALTAIR in the north or GeMS in the south). The resolution is $R \sim 5000$, over the full spectral range between the U and K bands. GMOX can pinpoint and collect deep spectra of regions with angular size as narrow as the spatial resolution of the HST. As shown in Figure 1, GMOX's 83 mas slit size ($f/16$), matching the 2-micron diffraction limit of Gemini (50 mas), resolves the scale of the inner Solar System at the distance of the Orion Nebula, $1/50$ th of a parsec at the distance of the LMC, half a parsec everywhere in the Local Group, 750 pc at redshift $z \simeq 1.5$. Beyond this distance the physical spatial resolution increases again with the angular distance, i.e. GMOX can resolve spatial scales less than 750 pc at all cosmological distances (Fig. 1). GMOX can thus spatially resolve any average galaxy in the observable Universe, according to the measured size-redshift relation (Fig. 2). At GEMS ($f/32$) the minimal slit size is narrower by a factor of 2. It is obvious that an instrument with these capabilities, standing above its predecessors in nearly all performance metrics based on combinations of sensitivity, angular resolution, wavelength coverage and multiplexing capability, has **great scientific potential for almost any field of astronomy**. GMOX has recently participated to the Gemini Feasibility Study Phase, and is currently under further development (for more details on the GMOX Feasibility Study, the instrument opto-mechanical and optical design, see [1–3]).

Resolving galaxies through cosmic time is the main science case for GMOX. An instrument like GMOX can help us write new chapters in our quest for understanding how the first galaxies formed, how they assembled and controlled their stellar mass, fed their central black holes and generally evolved to create the rich phenomenology we observe in our local Universe, harboring stars and planetary systems germane to our own existence. This contribution highlights a subset of the open questions that we have identified as of foremost importance for the near future of astronomy. Starting from these key scientific goals we have derived a series of requirements that GMOX must satisfy and therefore we have shaped the instrument design accordingly. The ten key science questions we would like to address by developing GMOX are: 1) How rapid and patchy was the process of **reionization of the Universe**? Which sources are responsible for it? 2) When did the **first stars**

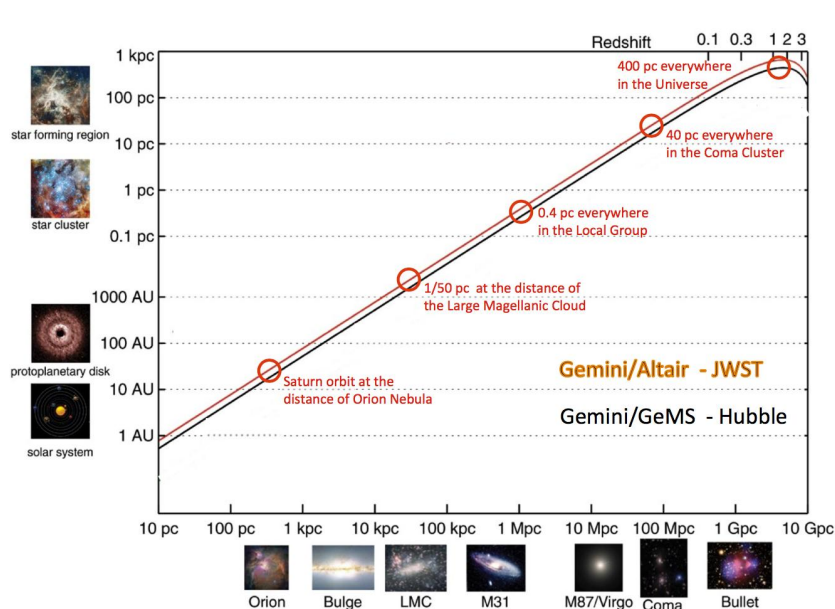


Figure 1. GMOX's capability to synthesize slits matching the diffraction limit of an 8m telescope allows one to analyze the physical status of compact regions across cosmic distances. The angular slit widths of GMOX at Gemini with ALTAIR and GeMS are marked in magenta and black, respectively; they are close to the diffraction limit at $\lambda = 2\mu\text{m}$ of the $D = 6.5$ m JWST telescope and of the $D = 2.4$ m HST. Major resolution thresholds are marked by red circles. (adapted from Fig. 4.1 of "From Cosmic Birth to Living Earth", AURA Report, 2015)

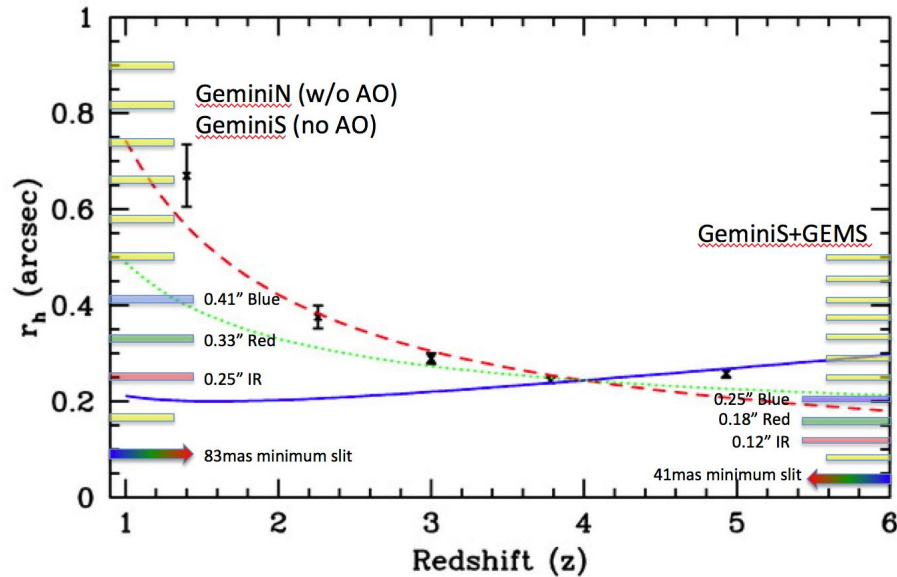


Figure 2. Size vs. redshift relation for Galaxies at $z > 1$ derived from the Hubble deep fields. The solid blue curve shows the expected trend in the WMAP cosmology if physical (proper) sizes do not evolve. The dashed red curve shows the trend if sizes evolve as $H^{-1}(z)$, and the dotted green curve shows $H^{-2/3}(z)$. The bars at the sides represent the slit sizes that GMOX can synthesize at $f/16$ (left) and at $f/32$ (right). The red, green and blue bars represent the nominal slits corresponding to a resolving power $R=5,000$. The colored arrows indicate the minimal slit width for the two configurations (adapted from [4]).

appear and what has been their role in **ending the Dark Ages**? 3) How did **Super Massive Black Holes** form? What are their seeds? 4) How do **Galaxies** build up their stellar mass? 5) What is the relation between star formation and **AGN**? 6) What is the origin of multiple stellar populations in **Globular Clusters**? 7) Is the **Initial Mass Function** Universal? 8) What are the connections between host galaxy properties, star Formation Rate density and **Cluster Formation, evolution and disruption**? 9) How does feedback from **Massive Stars** affect their birth environments? 10) What is the main driver of **Circumstellar Disks** evolution and dispersal? In this paper we describe how each of these questions can set a series of constraints on the instrument design and we conclude by deriving a global set of specifications for GMOX.

2. THE EARLY UNIVERSE: 3.5 GYR OF GALAXIES GROWTH

The first 3.5 Gyr of Cosmic History can schematically be divided in 4 phases: 1) The first 500 Myr, corresponding to $z > 10$, the “Dark-Ages”, when galaxies begin to form in dark matter halos created by initial density fluctuations in the primordial Universe and the first stars appear, starting the reionization of the Universe and producing the first metals; 2) The epoch of reionization, completed about one billion years after the Big Bang, corresponding to about $6 < z < 10$. In this epoch mini-halos expand and merge while the early compact embryos of present day galaxies are assembled. Super Massive Black Holes also have formed by the end of this phase; 3) The second billion years, $3 < z < 6$, where the stellar mass of the Universe grows from $\sim 1\%$ of its present value to $\sim 10\%$ with significant enhancement of heavy elements. Globular Clusters and the Milky Way Bulge are formed; 4) The “high noon”, between 2 and 6 billion years of cosmic history ($1 < z < 3$), when galaxies build about 75% of their stellar mass as the star formation efficiency reaches a maximum about 3.5 Gyr after the Big Bang. Because of cosmological redshift, these phases can be associated to different spectroscopic tracers of ionized hydrogen. This is indicated in Fig. 3, providing a visual guide to the following sections where we briefly examine each cosmic phase separately.

2.1 Dark ages and Population III objects

Open problems: The “Dark Ages”, i.e. the time interval between cosmic recombination ($t \simeq 0.4$ Myr after the Big Bang, $z \simeq 1100$) and the beginning of reionization ($t \simeq 500$ Myr, $z \simeq 10$), is the ultimate frontier of observational astronomy. Models predict that following recombination, the first dark matter halos begin to form driven by the density fluctuations imprinted in the primordial Universe. These halos grow by accretion increasing their virial temperature while the expanding neutral Universe cools down. Eventually the environment becomes cool enough that H_2 can radiate, allowing density to increase, up to the appearance of the first Population III (Pop III) stars at $z \sim 20 - 50$. These pure H-He stars are likely very massive, and are obvious candidates for

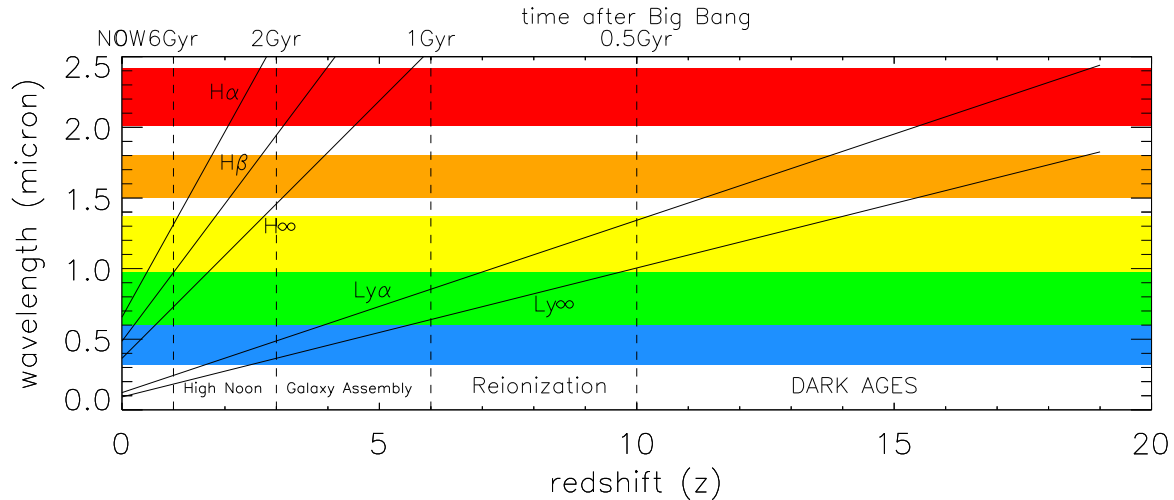


Figure 3. Illustration of how the main recombination lines of hydrogen scan the spectral range covered by GMOX as a function of cosmological redshift z . The colored bands refer to GMOX's Blue arm (blue), Red arm (green), NIR arm-J channel (yellow), NIR arm-H channel (orange) and NIR arm-K channel (red).

beginning the reionization of the Universe and the first metal enrichment. We don't know when they formed, how many, their IMF, the clustering properties, the lifetime, the efficiency of production and escape of hard-UV photons. The first galaxy seeds may appear soon after the first stars, still at redshift $z > 10$. Finding these primordial objects, either as massive hypergiants, clusters or galaxy embryos, is a holy grail of present day astrophysics. Analyzing them is the main science driver of JWST. At $z > 10$ the Universe is still opaque to $\text{Ly}\alpha$ radiation. Thus, the search for primordial objects has to be done using the Lyman-break technique beyond $\simeq 1 \mu\text{m}$, mostly with HST/WFC3-IR. Deep HST imaging in the F125W, F140W and F160W filters has provided so far only two candidates: the CLASH object in cluster MACS0647 [5] and the UDF j-39546284 object [6]. While the former appears to be multi-lensed and compatible with a geometrical solution for its $z \sim 10.8$ redshift and lens model, the second, initially found as a F125W dropout, has been later classified as a F140W dropout [7], that would push it at $z \sim 11.7$. However, its relatively bright flux and the fact that it is marginally resolved by HST suggests that this system may actually be a strong line emitter at $z \sim 2 - 3$.

Observational Needs: Extremely-high redshift objects are expected to be faint and rare, and therefore their search will probably remain a prerogative of JWST, with substantial investment of observing time. Predictions are model dependent, for example [8] estimate that JWST/NIRCam may return 5 galaxy candidates at $z > 10$ over its $\sim 10 \text{ arcmin}^2$ field. Projects like LSST, with the capability of reaching a shallower limiting depth $z \simeq 26.2 \text{ mag}$ can probe into the bright tail of this redshift range, providing a few hundreds of bright candidates ($M_{\text{AB}} \simeq 25$) across the sky. Spectroscopic confirmation will be needed to discriminate against low redshift sources, as samples of Lyman dropouts identified using broad near-IR filters have low- z interlopers caused by the Balmer/4000Å jump (cold stars and brown dwarfs may also be contaminants, depending on the filter set used). Deep spectroscopic observation may require substantial investment of exposure time (27 hours have been used by the MUSE team on VLT to reach a limiting flux $1 \times 10^{-19} \text{ erg s}^{-1} \text{ cm}^{-2} \text{ arcsec}^{-2}$, [9]). Detecting very-high redshift candidates discovered by JWST will require reaching $M_{\text{AB}} \simeq 28 - 29$ in the near-IR with $\text{SNR} \simeq 1$ per resolution element, in order to detect the Ly-break and the UV continuum after rebinning. Exposures requiring several nights, possibly with AO, would still be comparable to the amount of time effectively invested by JWST to discover the candidates in a combination of IR photometric bands. Multiplexing capabilities seem needed to justify those substantial investments of observing time. They would be extremely useful when high- z candidates are found near to the critical line of lensing foreground clusters, as in the case of MACS0647, as one can acquire wide-band spectra of hundreds of lensing and lensed galaxies, complementing JWST imaging and photometry at longer wavelengths. Reconstructing the full SEDs of all sources in the field of galaxy clusters

adds enormous value to the deepest spectroscopic observations of individual sources at extreme redshifts. At near-IR wavelengths, spectral resolution $R \simeq 5,000(10,000)$ is needed to cover about 80% (90%) of the near-IR spectral range accessible from the ground without being impacted by strong sky emission lines. The spectra would confirm the presence of the Lyman break in the near-IR and the lack of lines in the blue continuum. While rest frame optical emission lines would be displaced at wavelengths longer than $\simeq 3 \mu\text{m}$, in the JWST regime, a spectral range including the K-band may allow detection of CIV $\lambda 1549$ at $z \lesssim 14.49$ and CIII] $\lambda 1909$ at $z \lesssim 11.6$, tracers of metal-enriched systems. Wide wavelength coverage is also vital to reject low- z contaminants through their [OIII] $\lambda 5007$ and H β $\lambda 4862$ emission (observable at $z \lesssim 3.8$ and $z \lesssim 3.9$ respectively). Another key observational tracer is the HeII $\lambda 1640$ line, a tracer of Pop III stars. With 10% of the strength of Ly α line, the detection of this line provides the strongest evidence in support of the evanescent (a few Myr) Pop III sources.

2.2 Reionization and early galaxy formation

Open problems: As the Universe expands, the fraction of ionized atoms increases due to the Lyman continuum photons of primordial sources. This process is controlled by a few key parameters: the star formation rate density, $\rho_{SFR} [\text{M}_{\odot} \text{ yr}^{-1} \text{ Mpc}^{-3}]$, the rate of ionizing photons produced per unit mass $\xi_{ion} [\text{s}^{-1} \text{ M}_{\odot}^{-1}]$, and the fraction of those photons that escape to ionize the neutral intergalactic medium, f_{esc} . The product of these three values determines the fraction of ionized hydrogen in the Universe. The estimate of ρ_{SFR} relies on the luminosity functions of galaxies observed at high redshifts, either in their rest-frame UV or IR, extrapolated beyond our current sensitivity levels. The fact that the visibility of the Ly α line drops significantly beyond redshift $z = 6$ indicates that at that redshift, about 1 Gyr after the Big Bang, reionization is nearly complete. The problem is to explore beyond this limit to understand how reionization occurred.

At redshift $z < 10$ the Ly-break enters the visible range while Ly α shifts to the J-band (Fig. 3). Ground-based facilities therefore start to play a major role, complementary to HST and Spitzer, and, in the future JWST. So far, more than 1000 candidates have been found using HST data, but only 20 galaxies have been spectroscopically confirmed at $z > 6.5$ (with the record holder being at $z = 8.7$, [10]) almost exclusively on the basis of the presence of Ly α emission at $\lambda \sim 1.1 \mu\text{m}$. Using MOSFIRE at Keck-1 with $0.7''$ slits and a dispersion of $\simeq 1.2 \text{ \AA pix}^{-1}$, [11] could not detect Ly α emission in any candidate at $z \sim 7 - 9$ down to median limiting fluxes of $0.4 - 0.6 \times 10^{-17} \text{ erg s}^{-1} \text{ cm}^{-2}$ (5σ), whereas a few detections would have been expected if the distribution of Ly α emission had been the same as at ~ 6 . High redshift galaxies are elusive. The scarcity of $z \sim 8$ galaxies suggests either a dramatic increase in Ly α optical depth or that the number of star forming galaxy increases rapidly at redshift ~ 7 . Measures of the Thomson optical depth τ from Planck LFI polarization data, together with lensing and high-multipole temperature data, imply a reionization optical depth $\tau = 0.066 \pm 0.012$. This suggests that faint, star-forming galaxies are the main sources driving the reionization of the Universe, making reionization a quick process, with the Universe passing from 20% to 90% of ionized hydrogen in the 400 Myr between $6 < z < 9$ [8]. In this “late” scenario, Pop III stars may continue to form down to relatively low redshifts in isolated pockets of primordial gas, [12]. Source CR7 of [13] is a Ly α emitter at redshift of $z = 6.604$ presenting only a narrow HeII $\lambda 1640$ emission line (no other lines detected) in its X-shooter spectrum, which covers the spectral range from the U to the K band. HST/WFC3 observations show that CR7 is indeed spatially separated between a very blue component, coincident with the Ly α and He II emission, and two red components ($\sim 5 \text{ kpc}$ away), which dominate the mass. These findings are consistent with theoretical predictions of a Pop III wave, with Pop III star formation migrating away from the original sites of star formation (Fig. 4). Finding Pop III systems may eventually be not too hard: we just need to look at redshift $6 < z < 10$!

A complementary approach to the study of reionization requires studying the intergalactic medium (IGM) to determine when and how it became reionized. Quasar (QSO) spectra provide detailed information about the physical conditions of the IGM, and therefore play a central role in reionization studies. The structure of the Ly α forest generally confirms that reionization was largely completed by $z \sim 6$, although the final stages may extend to $z \sim 5$ [14, 15]. Damping wing absorption in the spectra of the first $z \sim 7$ QSO, ULAS J1120+0641, also appears to favor a significantly neutral IGM [16, 17], and hence a late end to reionization; however, it is only one object, and the damping absorption is subtle and difficult to measure. At the same time, studies of QSO absorption lines can shed light on the formation of the first galaxies, constraining the effect of feedback processes at early cosmic times. The first attempts to study early metal enrichment and feedback at $z > 6$ have been made with optical and near-IR spectrographs such as X-shooter. These have demonstrated that metals

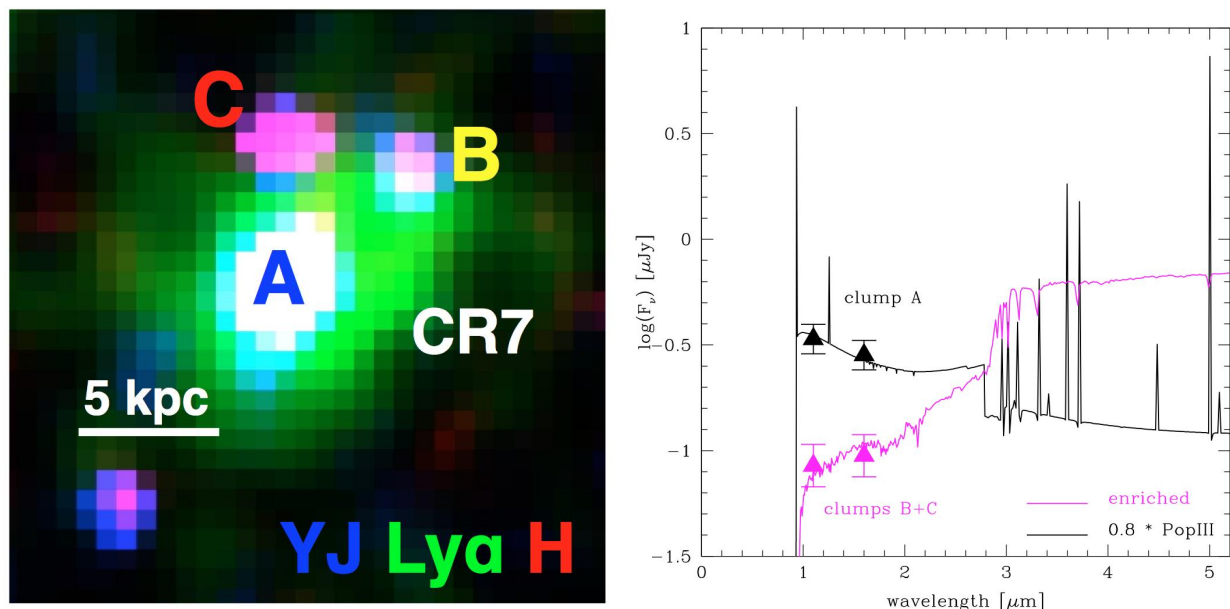


Figure 4. Left: reproduction of Fig.7 of [13]; a false color composite of CR7 using NB921/Suprime-cam imaging ($\text{Ly}\alpha$) and two HST/WFC3 filters: F110W (YJ) and F160W (H). Component A dominates the $\text{Ly}\alpha$ emission and the rest-frame UV light, whereas the (likely) scattered $\text{Ly}\alpha$ emission seems to extend all the way to B and part of C. Right: reproduction of Fig.8 of [13]; HST imaging in Y J and H allows one to model the resolved CR7 components with two very different stellar populations. While clump A is very blue and dominates the rest-frame UV flux, B+C are red and likely dominate the rest-frame optical and the mass. GMOX is designed to spectroscopically confirm this type of results.

are present in significant quantities at these redshifts, although in far less abundance than seen at later times. Current observations of metal absorbers traced by lines such as CIV, CII, OI, and MgII suggest a buildup of metals in the circum-galactic media of galaxies during the reionization epoch though from galactic winds, i.e., feedback processes that are critical for shaping these early galaxies. The current statistics are still fairly sparse, however, and it is not yet clear how rapidly the metals accumulate, or what population of galaxies they trace. Finally, observations of the CIV $\lambda 1549$ and MgII $\lambda 2798$ broad emission lines (redshifted in the NIR for QSOs at $z \sim 7$, place critical constraints on the mass of the black holes harbored in these powerful sources. Recent studies on the highest- z QSOs have shown that black holes with masses of $10^9 M_\odot$ are already in place when the Universe is less than 0.8 Gyr old (e.g., [16, 18, 19]). These findings pose serious issues on black hole seeds formation models. However, these results are based on the study of the brightest and highly accreting objects, and are most probable not representative of the whole QSO population. Increasing the number of known QSOs at $z > 6$ (there are ~ 70 QSOs known at $z \gtrsim 5.7$) would greatly improve our understanding of reionization and early galaxy assembly. We may have only probed "the tip of the iceberg" of the high- z QSO population, the bright, rare end of a more common, fainter population. This situation is set to change over the next several years as new quasars over $6 < z < 9$ will be discovered by DES, VISTA, LSST, WFIRST, and other survey facilities.

Observational Needs: So far, the analysis of spectral properties of distant galaxies has almost exclusively relied on SED fits to the HST photometry in the near-IR. Spectroscopy is needed to access the slope of the continuum: the UV galaxy luminosity has a spectral slope parameterized by $f_\lambda \propto \lambda^{-\beta}$. Typically, $\beta \simeq 2$ for star forming galaxies [20], and the spectrum is bluer, $\beta \sim 3$, for dust-free and primordial stellar populations, with some dependence on the IMF and the star formation history used to compute the SED. There are also several key physical diagnostics of star formation and gas dynamics that are available in the rest-frame UV (e.g., $\text{Ly}\alpha$, CIV, OVI,...) and that affect photometric analysis. Disentangling the effects of dust extinction from the contribution of emission lines to the underlying continuum is at the moment extremely difficult, given the uncertainties on the metallicity of these early systems. Spectroscopy is needed to enable calibration corrections for the emission

line fluxes as a function of redshift, improving both the stellar mass estimates and the characterization of how metallicity evolves with redshift. Spectroscopy is also essential to break the degeneracy in the SED fitting between massive/passive galaxies and star forming galaxies with strong emission lines, as both types tend to present similar signatures in broad-band photometry. As we have seen in the previous section, spectroscopic follow up of high redshift QSOs provides a formidable tool for analyzing the structure of the Universe at these early cosmic times. Study of the IGM through QSO absorption lines requires sensitive ($\text{SNR} > 10$, and preferably > 20), moderate to high-resolution optical and near-IR spectra of larger samples of $z > 6$ QSOs than are currently available. For reionization studies, the key observable is the strength and shape of the $\text{Ly}\alpha$ emission line. At $z > 7$ this requires near-IR spectra – primarily Y+J, but H and K are also critical for modeling the intrinsic, unabsorbed spectrum. Resolution of $R \sim 2000$ is sufficient, but $R > 4000$ is preferable for resolving discrete $\text{Ly}\alpha$ absorption lines in the QSO near zones, which affect the profile of the QSO $\text{Ly}\alpha$ emission. A sample size of $\sim 10 - 20$ QSOs at $z > 7$ would be excellent, which is in line with expectations from current NIR sky-surveys such as VISTA VHS. As discussed below, AO would be a major benefit for accessing faint targets, although smaller samples could be obtained in seeing-limited conditions. Intervening metal absorption lines are intrinsically narrow, and so higher resolution is needed ($R > 4000$) to study metal enrichment of the IGM. High SNR is also needed to detect weak lines ($\text{SNR} > 20$). At $z > 6$, the lines of interest fall over observed wavelengths of $\lambda = 9000 \text{ \AA}$ up through K band, so having optical + IR coverage is optimal. Current samples meeting these criteria in the near-IR are restricted to 6-7 objects at $z \sim 6$; an increase to 20+ objects is therefore needed. Extending to redshifts $z \geq 7$ is also a high priority. Due to the resolution and SNR requirements, particularly for fainter targets, AO would be a major asset for the suppression of the sky background and to minimize the impact of read noise and dark current (i.e., minimize the footprint of the spectral trace). In both cases, a southern location would be superior in order to follow up new high- z QSOs discovered in optical+IR sky surveys such as DES+VISTA, Pan-STARRS, and LSST, which are predominantly southern or equatorial. On longer term, targets will come from Euclid (all sky) and WFIRST (High Latitude Survey potentially in the south).

If Pop III objects can be found at lower redshift, a spectrograph with wide-band spectral coverage and high throughput at intermediate resolution is essential. The case of sources CR7 of [13] is emblematic: they used X-shooter, SINFONI and FORS2 at VLT, and DEIMOS at Keck, together with the original discovery images of the HST. Very wide band spectroscopy with VLT/X-shooter, from U to K, has been necessary to search for the presence of any emission lines other than $\text{Ly}\alpha$ and the $\text{He II}\lambda 1646$ line associated to Pop III stars. X-shooter, on the other hand, has been incapable of **spatially resolving** the individual components of this source: high spatial resolution is therefore the logical requirement to make a step forward. To analyze the UV slope, reaching the line-free continuum level of high-redshift galaxies in the near-IR, one has to use spectral resolution $R \gtrsim 3000$ to work between the OH lines. High throughput and the capability of synthesizing narrow slits are also required to boost sensitivity if AO are available. Study of the $\text{Ly}\alpha$ forest requires relatively high spectral resolution to disentangle metal lines, pushing again for spectroscopy with AO support to minimize losses and reach fainter sources. Field coverage of the order of a few arcmin is needed to map the $\text{Ly}\alpha$ absorption toward lensed objects on scales the order of 1 Mpc (comoving). Multi-object capability is again needed to justify long exposure times on faint sources, noting that cosmic variance becomes stronger at high redshift, increasing both the local source density and the need to sample multiple regions. As GMOX can provide a very precise estimate of the distance of hundred of sources in a field, it may enable one to trace the high frequency structure of the early Universe, clarifying where the first galaxies formed within the clumps of cosmic-web. GMOX has the potential to be transformative in the study of high- z QSOs, particularly if assisted by AO. Suppressing the sky background and minimizing the trace width on the detector will make it possible to obtain high-quality optical+NIR spectra of fainter objects than is currently possible with facilities such as VLT/X-shooter or Magellan/FIRE, hence enabling significantly larger samples to be obtained. The Vista VHS survey expects to uncover new QSOs at $z = 6 - 8$ down to $Y_{\text{AB}} = 21$. In AO mode it will be possible to obtain $\text{SNR} = 10$ spectra for such objects in 1.5 hours of exposure, and $\text{SNR} = 20$ in 5 hours. At $R \sim 5000$, GMOX will have sufficient resolution to study the IGM using the $\text{Ly}\alpha$ forest, as well as probe the environments of intervening galaxies through their metal absorption signatures. High throughput and the ability to suppress sky emission using narrow slits and AO will boost sensitivity, allowing one to obtain high-quality spectra of quasars out to $z \sim 8 - 9$, even as their $\text{Ly}\alpha$ emission shifts into the infrared. Multiply lensed QSOs can thus be used to probe the spatial structure and correlation of the $\text{Ly}\alpha$ clouds, with their filamentary structure, providing unique insights into the growth of cosmic structures.

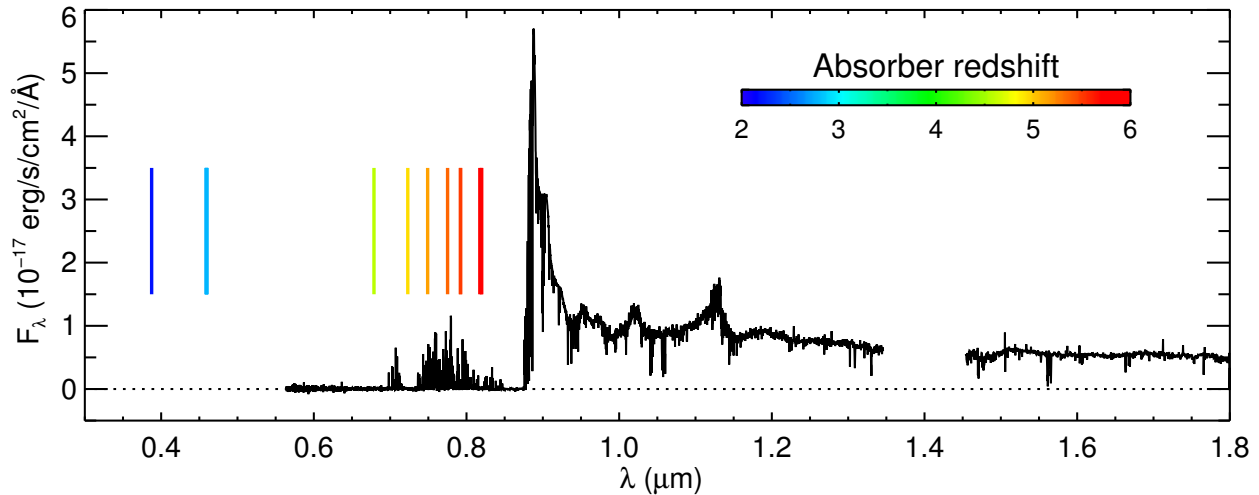


Figure 5. VLT/X-shooter spectrum of a quasar at $z = 6.3$. The Lyman- α forest is visible at $\lambda < 0.9 \mu\text{m}$, while metal absorption lines can be seen out into the near infrared. Wavelengths for Lyman- α at the redshifts of these absorbers, potentially corresponding to galaxies along the line of sight, are marked with vertical ticks.

2.3 Galaxy building epoch

Open problems: Between $3 < z < 6$, in the second billion year of cosmic history, galaxies begin to take shape increasing their stellar mass significantly through minor and major mergers, and gas accretion. This rapid process is accompanied by a substantial increase in heavy elements abundances. For the majority of galaxies, the star formation rate is proportional to the stellar mass of the galaxy. Also, the star formation rate surface density is proportional to the gas surface density (the Schmidt-Kennicutt law). This relation has a slope γ connected to the underlying physics of the scaling between star formation and cold gas. However, the Schmidt-Kennicutt Law does not appear to be “scalable” at all gas surface densities. In particular, at low gas surface densities, the SFR seems to change more rapidly than at high gas surface densities. This non-linear dependence suggests that star formation may have different modes, depending on the stellar mass, the environment, and on the accretion history of the galaxy (see also Sect. 3.1). Λ CDM models show that mergers of small satellites into larger galaxies is one of the main mechanisms of the hierarchical galaxy assembly. This is supported by the direct observations of fossil tidal features in galaxy groups: streams, tails, and bridges trace interactions that may have occurred several Gyr earlier. Understanding the formation and erasure of structures during the build-up epoch, the efficiency of cluster formation and the link between clusters and stellar mass functions requires spectroscopic observations of resolved galaxies at redshifts $z > 3$.

Observational Needs: Observationally, at $z \sim 4$ the Balmer/4000Å break enters the K-band while the Lyman break swings the visible portion of the spectrum, allowing one to identify thousand of galaxies [21–24]. Observing the features at UV and optical rest-frame wavelengths, one can select star-forming galaxies providing direct information on their most recent episodes of star formation. To assess the contribution of older stars, one has to move beyond $2\mu\text{m}$, to observe at near-infrared rest-frame wavelengths. While JWST will provide observations of such galaxies at long wavelengths, optical spectroscopy from the ground will be able trace their star formation rates in the last 100Myr, resolving localized starbursts. We expect that deep imaging of JWST/NIRCam will help to discover thousands of sources in this redshift range, calling for substantial parallel spectroscopic followup to derive precise redshifts and characterize the star formation activity, while eliminating low redshift interlopers.

The high density of sources in this redshift range is ideal for multi-object spectroscopy. GMOX must be able to cover deep fields of several arcmin^2 in a reasonable amount of time to match JWST/NIRcam search areas. This critical redshift range requires access to the full wavelength range, from the UV to the near infrared. GMOX

must provide such a spectral range, covering from the U-band (where the Ly- α line becomes accessible at $z \sim 3$) to the K-band (where the [OII] $\lambda 3727$ line, which is a tracer of star formation, is observable up to $z \sim 6$) in order to trace with continuity the evolution of star formation over the full redshift range. Resolution $R > 3,000$ provides accurate spectroscopic redshifts and assesses the contribution of line emission to the photometric fluxes for different classes of objects. Reaching the line-free continuum level of high redshift galaxies requires spectral resolution $R \gtrsim 4000$ to work between the OH lines. High throughput and the capability to synthesize narrow slits are also required to boost sensitivity. Study of the Ly α forest requires relatively high spectral resolution to disentangle metal lines.

2.4 “High noon” of cosmic history

Open Problems: Between $1 < z < 3$ galaxies experience a “growth spurt”, as the rate of mass buildup and AGN activity reaches its peak [25, 26]. To understand this phase of cosmic history we need to assess the SED of galaxies, not just globally, but resolving their substructures. Since galaxies are not homogeneous, it is critically important to discriminate between stellar populations of different ages, their contribution to the mass of the galaxies, the history of star formation, and the dust properties within the galaxies.

Observational Needs: The star formation rate can be traced by emission lines like H α and [OII] $\lambda 3727$ and by the rest-frame UV emission. Stellar masses can be derived by fitting the stellar continuum with SED models. From these synthetic spectra one can build a grid of observed stellar mass-to-light ratios as a function of D(4000) (i.e. the ratio of the flux density at 3850,3950Å to the flux density at 4000,4100Å; [27]), and the H δ absorption feature [28]. Having full access to different star formation rate indicators, consistently calibrated across a wide range of redshifts, would allow us to robustly derive how star formation changes within the galaxies. Minor mergers can provide a significant increase in galaxy size without a substantial stellar mass increase, leaving a well defined compact core of older star (e.g. [29]); vice-versa, adiabatic expansion powered by large-scale mass loss such as AGN feedback (e.g., [30]) can generate an expansion of the total stellar light profile. Discriminating between these two scenarios requires extreme AO to resolve galaxies bulges from disks, large field of view to compare several galaxies in a cluster and wide spectral coverage to map rest-frame indicators of stellar mass, age and star formation activity up to $z \sim 2$ (see contribution of S. Sweet at the 2015 Gemini Science Meeting). At even lower redshifts, the capability of taking wide-band spectra with high spectral and spatial resolution allows one to probe the origin and kinematics of stellar populations in normal, starburst, interacting, and active galaxies. A $\simeq 0.1''$ resolving power can probe scales of ~ 50 pc at the distance of Coma cluster. Enabling massive spectroscopy of resolved stellar populations in the nearest galaxies will revolutionize our understanding of stellar populations and probe the relationship between super massive black holes and their host galaxy.

Moderate spectral resolution ($R \sim 4000$) is needed to resolve broad emission lines associated with central AGN activity (e.g. H α , H β , CIV and MgII). The width of these broad emission lines combined with a measurement of the AGN continuum monochromatic luminosity can be used to estimate the mass of the powering black hole through scaling relations (e.g., [31]). Wide spectral coverage would allow one to track black-hole accretion and AGN activity throughout cosmic time. An instrument with such characteristics would be the perfect instrument to investigate the existing relation (if any) between AGN activity and galactic star formation. Wide spectral coverage and $R \sim 4000$ from the UV to the near IR is needed to measure the intensity of nebular emission lines (e.g., [O II] $\lambda\lambda 3727, 3730$, H β , [O III] $\lambda\lambda 4960, 5007$, H α , [NII] $\lambda\lambda 6548, 6584$, and [SII] $\lambda\lambda 6717, 6731$), stellar continuum, and absorption features (e.g., Balmer lines, CaII H and K, Mgb) as galaxies evolve over this redshift range. Resolution of a few thousand allows resolving Hydrogen emission lines to measure star formation rate and Balmer decrement (H α /H β), which provides a direct measurement of dust attenuation. These can be analyzed to yield dynamical information on the evolution of the disks, giving new insights into the inflow of material onto galaxies and the processes controlling star-formation in galaxies. The on-sky density of targets requires a multi-slit spectrograph. High spatial resolution is needed targeting single regions of enhanced star formation, measuring spectral variations across individual galaxies. Resolving power $R \simeq 5000$ (60 Km/s nominal) corresponds to a few km/s when the spectra are cross correlated. With such velocity resolution, it will be possible to probe into the properties and kinematics of galactic companions, constraining the frequency of satellite accretion and their relevance in the build up in the galaxy size and stellar mass.

3. THE LOCAL UNIVERSE

While Sect. 2 focused on cosmic scales, this section highlights some of the possible cases where an instrument like GMOX can help understand our Universe in finer details, down to the level of individual stars.

3.1 Galactic-Scale Star Formation

Open Problems: Star formation, the main process shaping galaxies from the cosmic dawn to present times, is *better described than understood* [32]. The missing link is the connection between the small scale of the single proto-star (~ 0.1 pc) and the large scale of extended star-forming structures and molecular complexes (several kpc). Galactic-scale star formation occurs in hierarchical structures of which bound star clusters occupy the densest peaks [33]. Star clusters can survive for even a Hubble time, as globular clusters, and provide a fossil record of the ancient star formation. The youngest massive clusters are easily detected to up to ~ 100 Mpc, and provide excellent tracers of current star formation. Hence, understanding cluster formation can provide a path for unraveling the physics of galactic-scale star formation, what regulates it, and its links to the properties and structures of the host galaxy. Young star clusters (YSCs), i.e. bound or semi-bound systems younger than ~ 100 Myr, are excellent tracers of recent star formation in all galaxies, and many of their properties have been studied over the past 10-15 years (see e.g. [34] and references therein); however a number of open questions remains. The reason why super-star-clusters, i.e. $\sim 10^6 M_\odot$ clusters, form in starburst galaxies (even dwarf ones) and mergers, but not in large spirals, remains a mystery, although the process is likely linked to ISM pressure and density (e.g. [35]). The cluster formation efficiency, i.e., the number of clusters formed per unit of star formation, appears to be a decreasing function of the star formation rate (SFR) surface density Σ_{SFR} , both locally and globally (Fig. 6), but available data are scant in the key range of very high and very low Σ_{SFR} , where models and predictions can be discriminated [36]. Adding to the uncertainties in the fact that most of the properties of YSCs are derived under the assumption of a universal stellar IMF, both at the low and high end, but evidence in this sense is contradictory [37–40]. The process of cluster disruption is also under hot debate. Two models have been put forward to explain the decline in number of bound clusters with age: mass independent disruption (MID, [41]) stating that the disruption timescale does not depend on mass and environment and that the number of clusters decreases with time simply following a t^{-1} relation, and mass dependent disruption (MDD, [42]) stating that the disruption of clusters depends on the initial mass of the cluster as well as on the environment of the cluster in the galaxy. Another fundamental question that has not yet been definitively addressed is related to the presence or not of an upper-mass truncation in the young star cluster mass function. Such a truncation is present in globular cluster populations and seems to be related to the galaxy where the population has formed [43]. However the results of the cluster mass function analysis of young star cluster populations in local galaxies are still contradictory [44, 45].

Observational Needs Many key questions related to the formation and evolution of young star clusters have not yet been answered because of the limited information we can access with imaging data. Conditions for the formation of super star clusters, cluster formation efficiency, and the IMF are best investigated in the youngest among the YSCs, i.e. those that are younger than ~ 10 Myr. This is because the youngest among the clusters are still closely linked to their natal environment, which is needed to garner insights into the open problems above. As an example, in order to probe the universality (or not) of the stellar IMF at the high end, young massive ($M \gtrsim 20 M_\odot$) stars still need to be present, i.e., the cluster needs to be very young. Almost all galaxies contain YSC populations, but these are best observed in the local Universe, where the YSCs can be isolated and measured amidst the galaxy background. However, starbursts and mergers are rare occurrences in the local Universe, thus placing a lower limit around ~ 100 Mpc in order to probe a large enough range of galactic environments (several ULIRGs and mergers are located within this volume). The key parameters to understand cluster formation and evolution are their masses and ages. Typically the age and other properties of the young (< 500 Myr) clusters are determined by SED fitting of UV and optical images. However, the determination of the age is hampered by the degeneracy between the age and extinction, i.e. red clusters could be young and reddened or old and not reddened. Disentangling age from dust attenuation, requires U-to-J SEDs. The Dn(4000) feature is a powerful age indicator, when coupled with the long wavelength leverage up to J, required to derive the dust geometry (see Fig. 7). Extinction determination is further aided by the availability of multiple hydrogen recombination

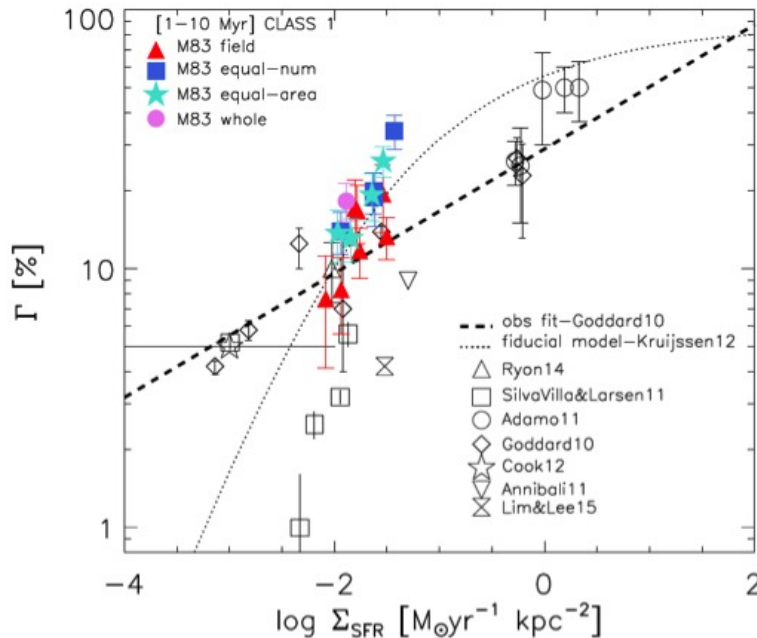


Figure 6. The cluster formation efficiency Γ , i.e., the ratio of cluster formation rate to the star formation rate, as a function of the SFR surface density Σ_{SFR} , for galaxies and galactic regions (from [34]). Only clusters younger than 10 Myr are included. The low and high Σ_{SFR} regions of the plot are not well defined by current data due to the difficulty of accessing this portions of the parameter space: the low end Σ_{SFR} is populated by dwarf galaxies, which require sensitive instruments, and the high end is populated by starburst galaxies, which are rare.

emission lines, e.g., $H\alpha$, $H\beta$, $P\beta$ [46]. Other age indicators will be observable thanks to the GMOX spectral coverage. For example, the $He\ II\ 4686$ (Wolf-Rayet feature) is created by Wolf-Rayet stars in clusters with typical ages of 4-6 Myrs, while the CO bandheads at $2.3\ \mu m$ are caused by red super giants dominating the spectra after the WR stars have disappeared. Ionizing photon fluxes are also required to determine the shape of the high end of the IMF. Extensions to wavelengths longer than J are required when dealing with natal clusters (< 2 Myr) which are still very embedded. Finally, cluster ages, which are derived from model-matching, are sensitive to the cluster metallicity, implying that metallicity measurements are required for accurate age (and mass, which depends on the age) determinations. Another important aspect which is still not fully constrained by observations is related to the effect of cluster feedback on the efficiency of gas removal from the region where the cluster has formed. Simulations are not able to remove gas from a cluster which has formed within a giant molecular cloud of $10^6\ M_{\odot}$ [47]. However, observational census of very young clusters in local galaxies shows that the central clusters are able to remove the left-over gas. It remains still to be answered which form of feedback is the most efficient: radiation pressure from very young massive stars, or mechanical feedback from stellar winds and supernovae explosions. By studying the emission lines of the H textscii regions around these young stellar clusters, the cluster feedback can be studied in detail, using the detection of lines with different ionization potential (e.g. $H\alpha$, SII, SIII, OIII and lines produced by shocks from the supernova ejecta like FeII).

GMOX needs to be able to obtain high quality spectra of large samples of young clusters in local group galaxies, allowing age determination via spectral fitting techniques [48]. This will give a significant improvement in the accuracy over the photometric determinations by resolving the degeneracy between age and extinction. The high spatial resolution is needed to isolate individual clusters. GMOX should have high multiplexing capability (200 - 500) to allow the spectral age determination of large samples of clusters in galaxies allowing the study of the environmental dependencies of the cluster properties and survival rate. Multi-object capabilities are the only way to efficiently observe YSC populations in external galaxies, where several hundreds to a few thousand YSC can be included within a field-of-view of $\sim 1' \times 1'$. To disentangle the age-extinction degeneracy, U-to-J coverage is needed. Masses are finally derived from the total flux at the long wavelengths ($> 7,000$ Angstrom, up to at least J-band). The broad wavelength coverage is also needed to enable age determination of clusters from 1 to up to ~ 10 Myr as several age dating features, emitted by stars of different ages, are covered in the spectrum: e.g. Balmer lines, Wolf-Rayet feature, CO-band heads (from red supergiants), Ca triplet, Mg lines. The use of adaptive optics is essential for this study in order to identify and isolate the individual clusters and to obtain as high a SNR as possible. A spectral resolution of 2000 is enough to identify the spectral features.

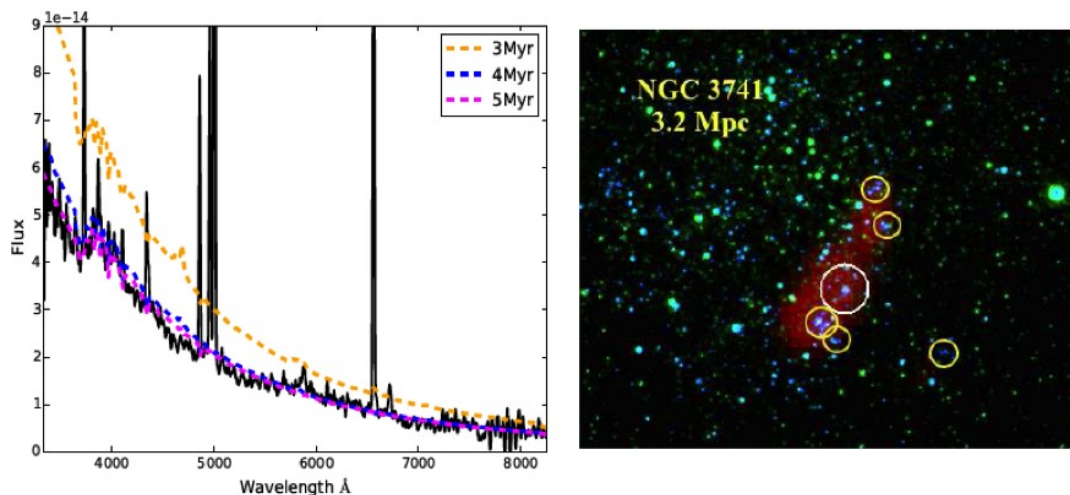


Figure 7. Left: Optical spectrum of a star cluster in a nearby dwarf galaxy, NGC3741 (shown at right, with a white circle), demonstrating how the wavelength coverage 3400-8000 is a minimal requirement to age-date clusters. Longer wavelength baselines are required in the presence of significant amounts of dust. Right: This color composite of NGC3741 shows that multi-object spectroscopy would be an efficient way to observe the clusters in this galaxy (yellow circles).

3.2 Massive star formation in Local Group Dwarfs

Open problems: The Local Group (LG) of galaxies offers the best opportunity to study massive stellar evolution and star formation (SF) in environments with a variety of properties, such as galaxy type, metallicity, gas density, dynamics and star formation history (SFH). SF modes and regulating factors as well as the interplay of stars and dust can be studied in detail given the vicinity of LG galaxies.[49] Ultimately, the resolved young populations of LG galaxies provide a crucial anchor point for the study of integrated properties of distant star forming galaxies. Given the typically low metallicities of dwarfs in the LG, they are ideal laboratories to study SF and evolution in conditions similar to the early Universe. They are indeed very important for understanding the efficiency of metal enrichment of the interstellar medium, which might differ between the LG spirals (Milky Way and M31) and dwarfs. A question arises whether the observed low metallicity in dwarfs reflects a quiet SFH or their inefficiency in retaining and mixing their own nucleosynthetic products.

Observational Needs: Massive stars are usually born in dense stellar environments, making it quite challenging to perform spectroscopy of individual objects (Fig. 8). Adaptive optics can provide the angular resolution needed in such crowded fields. Accurate spectral typing and estimates of stellar parameters are needed to construct H-R Diagrams. From the latter it is possible to estimate stellar masses and ages, thus characterizing the upper-end of the IMF in low-metallicity environments and the recent SFH. Given the typical size of these dwarf galaxies on the sky, 10s to 100s hot massive stars are present within 1 square arcminute, the exact value depending on the target dwarf galaxy. Other than the hot O and B stars, A-type supergiants can also be observed and their metallicities can be estimated from the many Fe lines available. These young stars reflect the *current* metallicity of their surroundings. Usually the star forming dwarf galaxies also present a number of cool red supergiants, which are slightly older than the hot OB stars. Covering the CaII triplet (8498, 8542, 8662 Å), visible in these stars, enables to estimate the metallicity of intermediate age populations and compare it to that of younger stars, thus quantifying their hosts' chemical enrichment.

Excellent image quality, typical of GLAO correction ($\simeq 0.3''$ in the visible) is needed to achieve the angular resolution needed to work in the crowded fields typical of nearby galaxies. A field of view of the order of 1×1 square arcmin is adequate to cover the typical extension of nearby dwarf galaxies. Medium resolution spectroscopy, $R \sim 3000$ is needed to show the presence of distinct populations, distinguishable by kinematics, metallicity and spatial distribution (as found e.g. in Sculptor Dwarf Spheroidal Galaxy but not in Carina).

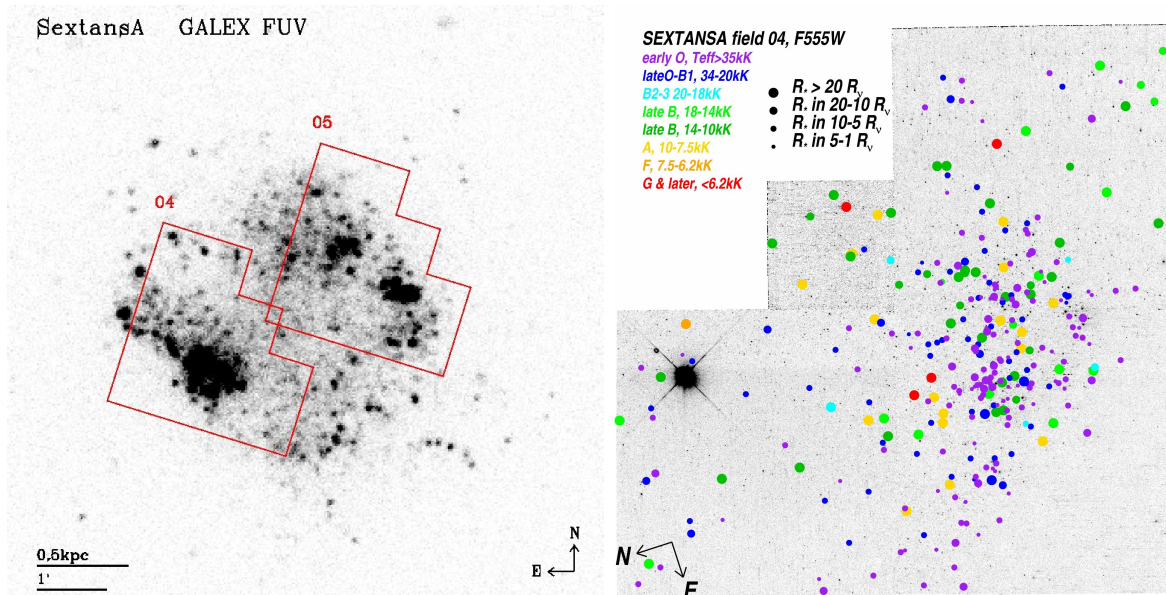


Figure 8. Left: GALEX image of the dwarf galaxy Sextans A, with the footprints of the HST/WFPC2 observations by [50, 51] superimposed. This galaxy represents a typical example of star-forming, low-metallicity, Local Group dwarf galaxy. Right: stellar temperature estimates from photometric SED fitting, by [50, 51]. HST observations like these can be used for GMOX target selection. The typical HST imaging cameras FoV can be covered with ~ 3 GMOX pointings.

3.3 Globular Clusters

Open problems: One of the most-obvious assumptions made by astrophysics for over half a century was to consider globular clusters (GCs) as: “*the purest and simplest stellar populations we can find in nature*” [52]. However, in the last few years an overwhelming body of observational evidence, both photometric and spectroscopic, has shown that this old, simplistic paradigm can’t be applied to most (if not all) GCs, [53]. Multiple generations of stars in GCs are now the rule rather than the exception. *De facto*, a new era in GC research has started. In the local Universe, GCs do not appear to be brewing multiple generation of stars [54], so special conditions, encountered only in the early Universe, may be instrumental for the occurrence of the GC’s multiple population phenomenon. Ultimately, studying and understanding how multiple stellar systems were born and have evolved in GCs will help us shading light on the series of events that characterized the early childhood of the Universe. Formally, all GCs exhibit multiple main sequences (MSs), and the most reasonable explanation is that stars in each of these MSs are characterized by a different Helium abundances [55]. Helium abundance cannot be directly measured by spectroscopy, except for high temperature, highly evolved stars [56]. Nevertheless, spectroscopic investigations of GCs have found large star-to-star variations in light-element (O, Na, Mg, Al and Si) abundances. These variations have distinct patterns: O and Mg abundances are positively correlated, and are anticorrelated with Na, Al and Si abundances. Such patterns leave little doubt about the chief nucleosynthesis culprit: high-temperature hydrogen fusion that includes CNO, NeNa, and MgAl cycles [57]. The main outcome of H burning, helium, is expected to be directly related to the observed chemical pattern of light elements in GCs. Stars on the MS that are highly enriched in He should have large depletions of O and Mg and large enhancements of Na and Al (possibly Si as well). In addition, first-generation stars are found to be O-rich, C-rich and N-poor. Conversely, second-generation stars, whose material has been CNO-cycle processed, are O-poor, C-poor and N-rich. The kinematic properties of different stellar populations represent another key piece of the puzzle for a complete picture of the formation and evolutionary history of GCs. According to a number of different formation scenarios [58–60] second-generation (2G) populations should form more concentrated in the GCs inner regions, and then slowly diffuse towards the outskirts, preferentially along radial orbits [61]. Even if formation and early dynamics did not produce strong differences in the kinematic properties of 1G and 2G populations, the effects of the long-term evolution driven by two-body relaxation, combined with the predicted (and observed) differences in the spatial distribution of 1G and 2G stars, can still leave significant fingerprints

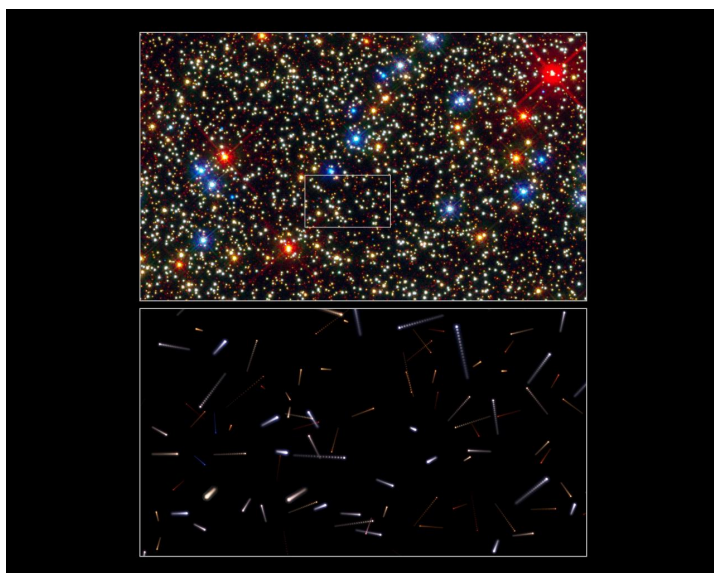


Figure 9. The upper panel shows a multi-color HST/WFC3 image of a field in the center of Omega Cen. The lower map shows the predicted positions of the stars highlighted by the white box. Each streak represents the motion of the stars over the next 600 years, sampled every 30 years. Radial velocity measures will allow one to reconstruct the 3d kinematics of the different stellar populations of the cluster.

in the current kinematic properties. However, line-of-sight velocities of GC stars have been measured so far only for the brightest giant stars. GMOX sensitivity and angular resolution will allow us to reach deep into the main sequence, giving us access to orders of magnitude more stars. Moreover, using only red giants represents a major limitation for studies focused on the global internal kinematics of GCs. In fact, because of the fast evolutionary timescale, giant stars have basically all the same dynamical mass, i.e. the mass of the current turn-off stars. It is only by reaching the main sequence that it would be possible to study the effects of energy equipartition, mass segregation and anisotropy [62]. When proper motions are also available for the same stars, GMOX line-of-sight velocities will allow us to constrain the 3D velocity and thus, the whole phase-space distribution functions, setting critical constraints on the dynamical and evolutionary status of the clusters. The core of GCs is the place where the most interesting dynamical interactions happen. Only state-of the art spectroscopy of faint stars in crowded fields will fully unlock these highly-demanding scientific investigations.

Observational Needs: Multiobject spectroscopy in the full visible range and with the capability of operating in crowded fields is ideally suited for studies of globular clusters. The apparent half-mass radius of most galactic globular clusters is about 1 arcmin, so field of views of this order are adequate for measuring hundred of stars in a single exposure. Because of crowding, high angular resolution is mandatory to target single sources down to the very center of GCs. Moderate resolving power ($R \gtrsim 3000$) from the near UV ($\lambda > 3400\text{\AA}$) to $1\text{ }\mu\text{m}$ is adequate to obtain spectra of turnoff and sub-Giant Branch stars in Galactic globular clusters, targeting e.g. CN (3883 \AA) and CH (4305 \AA) molecular bands to derive nitrogen and carbon abundances. Spectral resolution $R > 5000$ is needed to explore the close link between He enhancement and the simultaneous depletion/increase in light elements of faint stars on different main sequences. These targets can be photometrically selected and then spectroscopically analyzed to infer their light-element abundances. Near-UV capability would be especially useful to directly measure key CNO-cycle molecular bands: NH ($\sim 3400\text{\AA}$), CN ($\sim 3800\text{\AA}$, $\sim 4150\text{\AA}$), and CH ($\sim 4300\text{\AA}$). Near infrared coverage is needed to constrain the possible occurrence of cool, low-mass companions that may contaminate the results. By using narrow slits to increase resolving power and exploiting the wide spectral coverage it is possible to measure line-of-sight velocities. It should be possible to reaching the less massive MS stars and achieve higher precision than that achievable with proper motions from HST.

GMOX must be capable of collecting accurate high-resolution spectra of a few hundred stars in a single pointing. The field of view should be at least 1 square arcminute. The spectral coverage should range from the near-UV to the near-IR, resolution $R > 3500$.

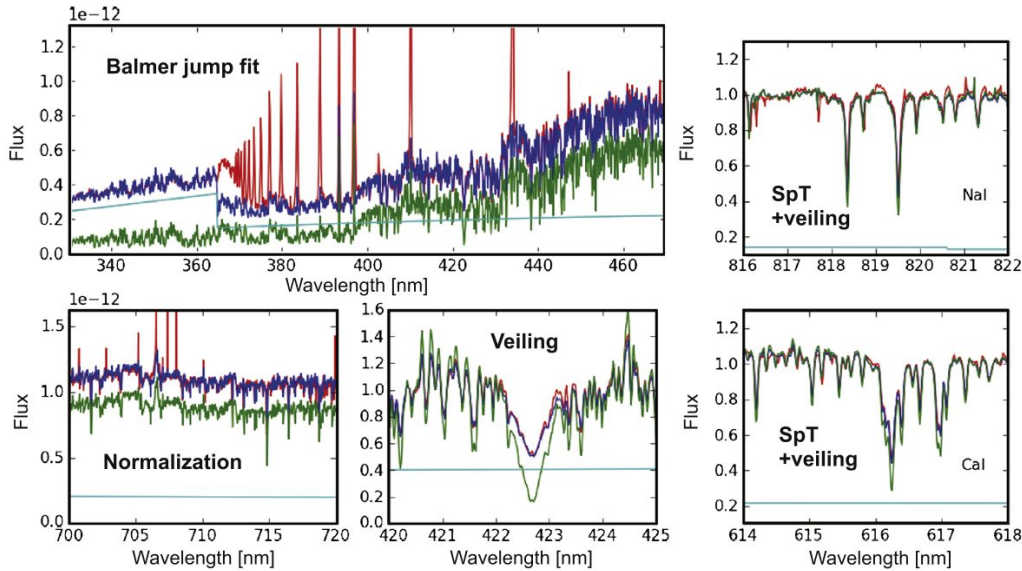


Figure 10. A combination of photospheric and accretion spectra can reproduce the observed emission; line veiling, however, affects the spectral features and biases the stellar type estimates. A global solution is necessary to properly derive the parameters of pre-main-sequence stars. (Adapted from [74]).

3.4 Star Formation and Circumstellar Discs

Open problems: Planets form in evolving protoplanetary disks around young stars located in young open clusters (YOCs) and star forming regions (SFRs). The evolution of the gaseous content of protoplanetary disks plays a key role in the planetary formation process (e.g. [63]). By studying disks around stars in galactic YOCs and SFRs of different age it is possible to infer what processes drive disk evolution. Two processes are thought to be the main drivers of disk evolution: viscous accretion and photoevaporative or disk winds [64]. Driven by turbulence, some disk material is accreted to the innermost regions while angular momentum is transported to the outer parts. At the hot, inner edge of the disk, ionized gas is funneled by the magnetic field to accrete onto the central star (magnetospheric accretion, see [65, 66]). Mass accretion gives rise to characteristic spectral signatures: a hot continuum, easily detected as an excess emission in the UV ($\lambda \lesssim 364$ nm) and as veiling across the entire visible region [67, 68], and strong and broad emission lines originated by the high velocity material infalling on the star [69]. The UV excess and the luminosity of the emission lines correlate with the total accretion luminosity (L_{acc}) [68, 70, 71]. However, disentangling photospheric spectrum from the accretion emission is not easy due to the opposite effect of accretion, which makes photospheric features shallower and the spectrum bluer, and extinction, which reddens the spectrum. On top of that, accretion is a highly variable process also on small timescales (minutes to hours, e.g., [72]). This has strong implications on non-simultaneous observations across different wavelength ranges. In practice, not only the estimated mass accretion rates but even the most fundamental stellar parameters (effective temperature, radius, luminosity) are often poorly defined, adding large scatter to the HR diagram of nearly coeval populations that in principle should nicely trace theoretical isochrones (with binaries). The availability of the X-shooter spectrograph at the 8m ESO/VLT telescope has helped astronomers shed some light on this issue. By covering the spectral range from $\lambda \sim 300$ nm to $\lambda \sim 2500$ nm simultaneously with high-sensitivity and medium resolution, X-shooter allows one to beat the degeneracies between the stellar and accretion parameters. The detailed analysis carried out by [73] of the broad X-shooter spectra of two apparently old (30 Myr) but accreting stars in the $\simeq 1$ Myr Orion nebula cluster (ONC) has shown that their correct stellar parameters places these targets in the same region of the HR diagram as the other stars in this region (see Fig. 11). The better determination of the stellar parameter was possible thanks to the large wavelength coverage of the spectra, leading to a better determination of both accretion and extinction, as well as the spectral type, of the targets. Similarly, [75] have used mostly Keck/LRIS spectra to show that spectral type classification of young stars is inaccurate if veiling due

to accretion is not quantified and considered together with extinction. The importance of covering a wide spectral range simultaneously is ultimately dictated by the very short timescales on which accretion varies, as short as minutes to hours [72]. An estimate of veiling on a non-simultaneous spectrum does not allow one to achieve the same precision in the determination of stellar parameters; this possibly is the main cause of the longstanding problem with the exceedingly large age dispersion in young clusters. The UV-excess is surely the most direct tracer of accretion, but the accretion luminosity, and thus the mass accretion rates, can also be derived using the luminosity of various emission lines. Recent works with X-shooter have demonstrated that robust estimates of accretion are obtained, once stellar parameters and extinction have been properly derived, combining the luminosity of multiple emission lines [76, 77]. The best correlation between line and accretion luminosity is found for high upper-level Balmer lines (e.g., $H\gamma$) in the blue part of optical spectra and Paschen series lines, such as the $Pa\beta$ line in the near-infrared. This line, as well as other near-infrared emission lines, are accurate proxies as their fluxes are less affected by extinction. Moreover, infrared spectroscopy can also be used to probe the substellar regime. The other main processes driving the evolution of protoplanetary disks are winds, which are best studied spectroscopically through the analysis of forbidden emission lines [78]. High-velocity components of forbidden lines trace jets while the low-velocity component traces slow disk winds, possibly photoevaporated by the high-energy (X-ray and UV) photons coming from the central star [79]. Studying forbidden lines in young stars allows one to determine the physical conditions of these winds, such as temperature and density [80]. Another important parameter to be considered, besides, age, is the effect of environment. Recent studies indicate that disk accretion last longer in environments with lower metallicity, such as in the outskirts of our Galaxy and in the Magellanic Clouds [81]. Such studies may lead to a connection between star and planet formation in our solar neighborhood and other galaxies throughout cosmic history. However, these results require confirmation, relying solely on photometric surveys and a single accretion indicator, the $H\alpha$ line, which is not the most accurate tracer of accretion. It is necessary to accurately determine stellar and accretion parameters of statistically significant samples of targets at different metallicity (i.e. in the Magellanic Clouds) using the same methodology described above for close-by targets.

Observational Needs: X-shooter is the best instrument available today to investigate the nature of pre-main-sequence objects, allowing one to determine self-consistently the Spectral Type, extinction and accretion luminosity, the jet/disk wind properties, and the relative importance of these processes. X-shooter, however, is limited by the lack of multi-object capability and operates only in the seeing limited regime. Great progress would be enabled by a wide-band multi-object spectrograph: young galactic clusters in the Milky Way reach extremely high density (about 30,000 stars/pc³ in the core of the Orion Nebula Cluster) and are therefore ideally suited for multi-slit spectroscopy. Wide band spectral coverage is needed to measure lines from different atomic species with different ionizing conditions, including H recombination lines (the entire Balmer and Paschen series as well as the higher transition Brackett series) and a large number of molecular transitions of H₂ and CO in the near-IR. Resolution should be adequate to resolve the broad $H\alpha$ line ($\Delta\lambda \simeq 100$ km/s) of classical T Tauri stars. Using extremely narrow slits allows one to study the central regions of clusters, characterized by strong and highly non-uniform background, and source crowding. It also allows one to increase spectral resolution to probe the kinematics of the inner regions close to the source of jets and outflows.

GMOX must have multi-slit capability over a field of view of at least one square arcmin. Very-wide band spectral coverage, U-to-K, allows one to measure the rich spectrum characteristic of young stellar objects. Resolution $R > 5000$ is needed to resolve the broad $H\alpha$ line tracing accretion and jets kinematics. The ability to select narrow slits ($\sim 0.1''$) with AO allows one to penetrate the inner regions of young clusters, minimizing confusion and background.

4. LSST TRANSIENTS

By probing 100 times more volume than the recent generations of transient searches such as Pan-STARRS1 and PTF, LSST is going to enable the next level of time domain studies, probing variability both in position and time. Rarely observed events will become commonplace, new and unanticipated events will be discovered. The impact of LSST on astrophysics has been recognized by the latest Decadal Survey; Gemini is expected to play a key role, in particular with the spectroscopic followup of transients. The most compelling case for LSST

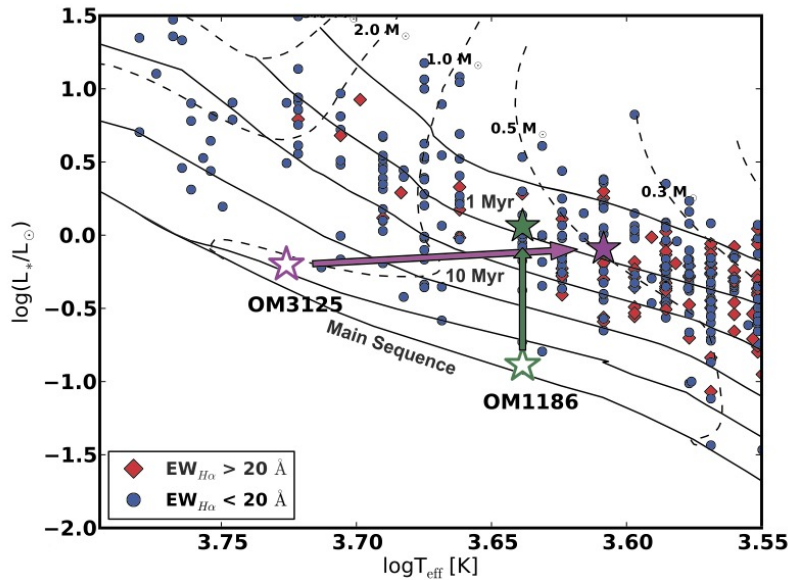


Figure 11. Position on the HR Diagram of the two objects in the Orion Nebula Cluster discussed in the text. The empty stars represent the target stellar parameters reported in the literature, while the positions determined with our method are shown with filled stars. The evolutionary tracks shown in the plot are by [82]. (Adapted from [73]).

follow-up with Gemini is probably provided by exotic sources that emerge from below the detection threshold, rising in brightness over time scales of hours, or a few days. One can refer to true transients as objects whose character is changed by the event, usually as the result of some kind of explosion or collision, whereas variables are objects whose nature is not altered significantly when they increase in brightness. The 5 or 6 band photometry of LSST will have limited predictive power to constrain the nature of enigmatic transients: medium resolution spectroscopy over a wide-band spectral range is absolutely needed.

A convenient way to represent the basic characteristics of explosive events is to plot the peak luminosity versus characteristic time scale. Figure 12 shows the location of some of them. The absolute magnitudes on the right can be composed with the distance modulus of the local Universe: long-period novae at $V_{\text{abs}} \simeq -7$ could be detected at their peak by LSST up to the distance of the Virgo cluster ($\text{DM}=+31$). Spectroscopic followup is within reach. Supernovae occupy the upper part of the diagram. The spectroscopic light curves of their expanding shells provides us with a 3-dimensional movie of the chemical enrichment of galaxies, including the production and decay of radioactive materials and dust grains which are a prerogative for the existence of life. Supernovae are also fundamental distance indicators and have provided the first direct evidence for cosmic acceleration [83,84]. This discovery rested on observations of several tens of supernovae at low and high redshift. These samples have been observed with a variety of telescopes, instruments, and photometric passbands. The low-redshift SN Ia measurements that are used both to anchor the Hubble diagram and to train SN Ia distance estimators are themselves compiled from combinations of several surveys using different telescopes and selection criteria. When these effects are combined with uncertainties in intrinsic SN Ia color variations and in the effects of dust extinction, the result is that the current constraints are largely dominated by systematic rather than statistical errors. An instrument allowing one to observe similar supernovae over a wide range of redshifts, minimizing background confusion from the host galaxies, would allow reduction of the systematic uncertainties that eventually propagate into our knowledge of fundamental parameters of the cosmos. Supernovae are also connected to the Gamma-ray bursts (GRBs), the most violent cosmic events associated with the birth of a rapidly spinning stellar black hole. Long duration GRBs probably result from the deaths of certain types of massive stars [85]. Since the explosion is mostly directional (jetted) with conical opening angles ranging from less than a degree to a steradian, a detection depends on the location of the observer. The initial emission of gamma rays is followed by an optical afterglow from the interaction of the relativistic debris and the circumstellar medium. An observer outside the cone of the jet misses the burst of gamma-ray emission, but can still detect the subsequent afterglow emission [86], an off-axis orphan afterglows. Since the beaming fraction (the fraction of sky lit by gamma-ray bursts) is estimated to be between 0.01 and 0.001, the true rate of GRBs is 100 to 1000 times the observed rate. Since a supernova is not relativistic and is spherical, all observers can see the supernovae that

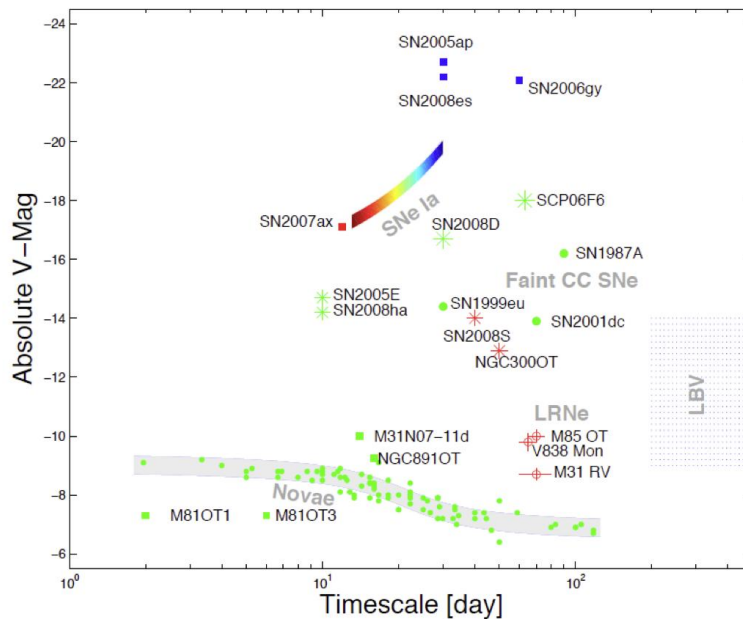


Figure 12. Peak V-band luminosity of known transients, either explosive (supernovae) or eruptive (novae, luminous blue variables - LBVs), as a function of duration, color coded to represent the true color at maximum brightness. Also shown are other peculiar transients (reproduction of Fig.8.1 of LSST Science Book)

accompany GRBs. Understanding the nature of GRBs is another fascinating program that can be attacked by a sensitive wide-band spectrograph at Gemini.

Observational Needs The next generation spectrograph for the Gemini telescope should be able to operate over a very-wide spectral range covering the visible bandpasses, where LSST operates, with extension to the infrared, as dictated by both AO performance and cosmological redshift. The spectra of e.g. supernovae are extremely rich of emission lines, like e.g. $H\alpha$, HeI 5570, 10830, Ci 8729, 9812, OI 5577, 6300, 6364, MgI 4571, $SiII$ 10990, 16450, Si 10824, 11309, $CaII$ 7292, 7325, 8499-8663, $FeII$ 7155, 12570, 15330, 16400, $CoII$ 15430. To track the rest frame optical spectrum up to $z \simeq 2$, beyond the limit of the furthest supernova discovered by the HST, one has to reach the K-band with spectral resolution adequate to reject OH lines.

To trace light curves, the spectrograph must be stable and allow for accurate, absolute spectrophotometric calibration. The ability to rapidly acquire a target minimizes overhead, in particular for programs dealing with relatively bright targets of opportunity or long term monitoring programs, reducing the impact on regularly scheduled observations. Multi-object capability is always a plus, allowing one to e.g. identify the host galaxy if a supernova appears in a remote cluster. Temporal resolution is also a plus, and readout times as short as a few seconds may represent an interesting capability for certain types of transients, like e.g. planetary transits.

5. SUMMARY OF GMOX SCIENCE REQUIREMENTS

As expected for a multi-purpose facility instrument like GMOX, the top-level requirements have been derived not just from a single application case but from a *set* of compelling science cases, taking into account the technical constraints provided by the facilities to be used (Gemini, GeMS) and the current status of technology (DMDs, detectors). In the following, we summarize the science driven requirements for GMOX.

Spectral Coverage: Extra-wide spectral coverage, from the U-band to the K-band accessible from the ground, emerges as a general requirement. It allows for better science by measuring multiple spectroscopic tracers of each target, disentangling the role played by the various regions contributing to the spectrum. Continuous spectral coverage allows measuring/recovering the redshift of sources with missing or mediocre estimates, e.g. from photo- z methods, and in general to trace similar physical phenomena across cosmic history. Simultaneous coverage is a huge advantage in terms of observing efficiency, but there are cases involving the study variable objects, like transients or accreting Pre-Main-Sequence stars, where simultaneity is scientifically needed. Simultaneous, wide spectral coverage also provides significant advantages from the operational point of view, as one instrument can

be permanently mounted at the telescope and overhead is minimized. It also allows one to optimally exploit the best seeing conditions and bright vs. dark time. Our nominal spectral range will be from 350nm to 2.4 μ m.

Multi-object capability: This capability facilitates another huge gain in observing efficiency. In principle, IFUs are a possibility but they do not cover an extended spectral range AND a wide field of view with high spatial resolution at a reasonable cost. Other more conventional approaches (reconfigurable slits, lenslets) are not well matched to the sharpness provided by extreme adaptive optics at an 8 m telescope, and to the variety of conditions that may be encountered, from poor seeing to extreme Strehl ratio. Therefore, our approach is to use MEMS devices, in particular the Digital Micromirror Devices made by Texas Instruments, as they are commercially available at low cost, are extremely reliable and have pristine cosmetic quality. Using a single DMD per spectrograph arm GMOX can easily take $\simeq 400$ full, well separated spectra in parallel with extremely rapid and accurate target acquisition.

Sensitivity: Exploiting AO allows one to reach the ultimate sensitivity achievable from the ground. Spectroscopy in the nearly diffraction limited regime enables the use of extremely narrow slits, reducing the noise due to the sky background to minimum levels. To work with adaptive optics, the spectrograph must be capable of synthesizing and aligning slits of a few micron, matching the diffraction limit of the telescope $\lambda/D = 25$ mas at 1 μ m). Keeping the field of view entirely within the unvignetted field of view of Gemini (3'1) is also important to minimize thermal background in the K-band. Again, DMDs appear ideally suited for this application.

Efficiency: To reach the faintest sources, the highest possible throughput must also be pursued. The optics and detectors will therefore require different optimization vs. wavelength and slit sizes. For this reason we envision three spectroscopic arms: Blue (350-589 nm), Red (589-1000 nm, cut at the GeMS laser wavelength) and NIR, the last being split into three channels to cover the Y+J, H and K bands. Also the capability of acquiring a multitude of sky-spectra adjacent to each target, essential for accurate sky-subtraction, provides de-facto and increase by a factor of two in efficiency over systems requiring beam-switching.

Spectral Resolution: A resolving power of about $R = 5,000$ emerges as a general requirement. On the other hand, for a slit spectrograph the resolving power is not a fixed parameter, as it depends on the slit width selected by the user. Optimal sampling of the slit on the detector (about 3 pixels/slit) can be achieved only at a central, "nominal" value of the slit width. Narrowing the slit one achieves higher spectral resolutions at the expense of worse sampling, and viceversa. For a Gemini facility instrument, this means that the resolving power may depend on the observing conditions, since to exploit the AO to reach the faintest sources one will use narrow slits thus increasing spectral resolution. We have made the assumption that in 2022 Gemini will routinely operate with some level of AO correction. We have therefore set our nominal resolving power $R \simeq 5000$ for a slit width of 0.25" in the infrared, 0.33" in the Red channel, and 0.41" in the Blue channel. These values generally correspond to what can be routinely achieved with limited AO performance, e.g. with ground layer correction, or in laser-only mode (no tip-tilt).

ACKNOWLEDGMENTS

D. Apai (U. Arizona), S. Beckwith (Berkeley), S. Heap (NASA-GSFC), M. Kasper (ESO), S. Kassin (STScI), J. Mather (NASA Goddard), A. Miotello (Leiden), A. Rest (STScI), K.B. Schmidt (AIP), M. Stiavelli (STScI), D. Vorobiev (RIT) and F. Zerbi (INAF) are especially acknowledged for key insights on the capabilities of GMOX.

We would like to thank the Gemini Observatory for funding the GMOX feasibility study under contract agreement number N506722. In addition, we would like to express our appreciation to Stephen Goodsell, Madeline Close, Ruben Diaz, Pascale Hibon, Scott Kleinman, Rachel Mason, Vanessa Montes, William Rambold, Bernadette Rambold, and Chad Trujillo, for their many constructive comments and insight throughout the feasibility study process. The Gemini Observatory is operated by the Association of Universities for Research in Astronomy, Inc., under a cooperative agreement with the NSF on behalf of the Gemini partnership: the National Science Foundation (United States), the National Research Council (Canada), CONICYT (Chile), the Australian Research Council (Australia), Ministrio da Cincia, Tecnologia e Inovao (Brazil) and Ministerio de Ciencia, Tecnologia e Innovacin Productiva (Argentina).

REFERENCES

- [1] Robberto, M., Smee, S., Barkhouser, R., Ninkov, Z., Gennaro, M., and Heckman, T. M., “Feasibility study of GMOX: a next-generation instrument for Gemini,” in [*Ground-based and Airborne Instrumentation for Astronomy VI*], *Proc. SPIE* **9908** (July 2016).
- [2] Smee, S. A., Barkhouser, R. H., Robberto, M., Ninkov, Z., Gennaro, M., and Heckman, T. M., “The opto-mechanical design of GMOX: a next-generation instrument concept for Gemini,” in [*Ground-based and Airborne Instrumentation for Astronomy VI*], *Proc. SPIE* **9908** (July 2016).
- [3] Barkhouser, R. H., Robberto, M., Smee, S. A., Ninkov, Z., Gennaro, M., and Heckman, T. M., “The optical design of GMOX: a next-generation instrument concept for Gemini,” in [*Ground-based and Airborne Instrumentation for Astronomy VI*], *Proc. SPIE* **9908** (July 2016).
- [4] Ferguson, H. C., Dickinson, M., Gialalisco, M., Kretchmer, C., Ravindranath, S., Idzi, R., Taylor, E., Conselice, C. J., Fall, S. M., Gardner, J. P., Livio, M., Madau, P., Moustakas, L. A., Papovich, C. M., Somerville, R. S., Spinrad, H., and Stern, D., “The Size Evolution of High-Redshift Galaxies,” *ApJ* **600**, L107–L110 (Jan. 2004).
- [5] Coe, D., Zitrin, A., Carrasco, M., Shu, X., Zheng, W., Postman, M., Bradley, L., Koekemoer, A., Bouwens, R., Broadhurst, T., Monna, A., Host, O., Moustakas, L. A., Ford, H., Moustakas, J., van der Wel, A., Donahue, M., Rodney, S. A., Benítez, N., Jouvel, S., Seitz, S., Kelson, D. D., and Rosati, P., “CLASH: Three Strongly Lensed Images of a Candidate $z \approx 11$ Galaxy,” *ApJ* **762**, 32 (Jan. 2013).
- [6] Bouwens, R. J., Illingworth, G. D., Labbe, I., Oesch, P. A., Trenti, M., Carollo, C. M., van Dokkum, P. G., Franx, M., Stiavelli, M., González, V., Magee, D., and Bradley, L., “A candidate redshift $z \sim 10$ galaxy and rapid changes in that population at an age of 500 Myr,” *Nature* **469**, 504–507 (Jan. 2011).
- [7] Ellis, R. S., McLure, R. J., Dunlop, J. S., Robertson, B. E., Ono, Y., Schenker, M. A., Koekemoer, A., Bowler, R. A. A., Ouchi, M., Rogers, A. B., Curtis-Lake, E., Schneider, E., Charlot, S., Stark, D. P., Furlanetto, S. R., and Cirasuolo, M., “The Abundance of Star-forming Galaxies in the Redshift Range 8.5–12: New Results from the 2012 Hubble Ultra Deep Field Campaign,” *ApJ* **763**, L7 (Jan. 2013).
- [8] Robertson, B. E., Ellis, R. S., Furlanetto, S. R., and Dunlop, J. S., “Cosmic Reionization and Early Star-forming Galaxies: A Joint Analysis of New Constraints from Planck and the Hubble Space Telescope,” *ApJ* **802**, L19 (Apr. 2015).
- [9] Bacon, R., Brinchmann, J., Richard, J., Contini, T., Drake, A., Franx, M., Tacchella, S., Vernet, J., Wisotzki, L., Blaizot, J., Bouché, N., Bouwens, R., Cantalupo, S., Carollo, C. M., Carton, D., Caruana, J., Clément, B., Dreizler, S., Epinat, B., Guiderdoni, B., Herenz, C., Husser, T.-O., Kamann, S., Kerutt, J., Kollatschny, W., Krajnovic, D., Lilly, S., Martinsson, T., Michel-Dansac, L., Patricio, V., Schaye, J., Shirazi, M., Soto, K., Soucail, G., Steinmetz, M., Urrutia, T., Weibacher, P., and de Zeeuw, T., “The MUSE 3D view of the Hubble Deep Field South,” *ArXiv e-prints* (Nov. 2014).
- [10] Zitrin, A., Labbe, I., Belli, S., Bouwens, R., Ellis, R. S., Roberts-Borsani, G., Stark, D. P., Oesch, P. A., and Smit, R., “Lyman-alpha Emission from a Luminous $z=8.68$ Galaxy: Implications for Galaxies as Tracers of Cosmic Reionization,” *ArXiv e-prints* (July 2015).
- [11] Treu, T., Schmidt, K. B., Trenti, M., Bradley, L. D., and Stiavelli, M., “The changing $\text{Ly}\alpha$ optical depth in the range $6 < z < 9$ from the MOSFIRE spectroscopy of y-dropouts,” *ApJ* **775**(1), L29 (2013).
- [12] Trenti, M., Stiavelli, M., and Michael Shull, J., “Metal-free Gas Supply at the Edge of Reionization: Late-epoch Population III Star Formation,” *ApJ* **700**, 1672–1679 (Aug. 2009).
- [13] Sobral, D., Matthee, J., Darvish, B., Schaerer, D., Mobasher, B., Röttgering, H. J. A., Santos, S., and Hemmati, S., “Evidence for PopIII-like Stellar Populations in the Most Luminous Lyman- α Emitters at the Epoch of Reionization: Spectroscopic Confirmation,” *ApJ* **808**, 139 (Aug. 2015).
- [14] Fan, X., Strauss, M. A., Becker, R. H., White, R. L., Gunn, J. E., Knapp, G. R., Richards, G. T., Schneider, D. P., Brinkmann, J., and Fukugita, M., “Constraining the Evolution of the Ionizing Background and the Epoch of Reionization with $z \sim 6$ Quasars. II. A Sample of 19 Quasars,” *AJ* **132**, 117–136 (July 2006).
- [15] Becker, G. D., Bolton, J. S., Madau, P., Pettini, M., Ryan-Weber, E. V., and Venemans, B. P., “Evidence of patchy hydrogen reionization from an extreme $\text{Ly}\alpha$ trough below redshift six,” *ArXiv e-prints* (July 2014).
- [16] Mortlock, D. J., Warren, S. J., Venemans, B. P., Patel, M., Hewett, P. C., McMahon, R. G., Simpson, C., Theuns, T., González-Solares, E. A., Adamson, A., Dye, S., Hambly, N. C., Hirst, P., Irwin, M. J., Kuiper, E., Lawrence, A., and Röttgering, H. J. A., “A luminous quasar at a redshift of $z = 7.085$,” *Nature* **474**, 616–619 (June 2011).
- [17] Bolton, J. S., Haehnelt, M. G., Warren, S. J., Hewett, P. C., Mortlock, D. J., Venemans, B. P., McMahon, R. G., and Simpson, C., “How neutral is the intergalactic medium surrounding the redshift $z = 7.085$ quasar ULAS J1120+0641?,” *MNRAS* **416**, L70–L74 (Sept. 2011).
- [18] De Rosa, G., Venemans, B. P., Decarli, R., Gennaro, M., Simcoe, R. A., Dietrich, M., Peterson, B. M., Walter, F., Frank, S., McMahon, R. G., Hewett, P. C., Mortlock, D. J., and Simpson, C., “Black Hole Mass Estimates and Emission-line Properties of a Sample of Redshift $z \gtrsim 6.5$ Quasars,” *ApJ* **790**, 145 (Aug. 2014).

- [19] Wu, X.-B., Wang, F., Fan, X., Yi, W., Zuo, W., Bian, F., Jiang, L., McGreer, I., Wang, R., Yang, J., Yang, Q., Thompson, D., and Beletsky, Y., "Discovery of a 12 billion solar mass black hole at redshift 6.3 and its challenge to the black hole/galaxy co-evolution at cosmic dawn," *IAU General Assembly* **22**, 51223 (Aug. 2015).
- [20] Meurer, G. R., Heckman, T. M., and Calzetti, D., "Dust Absorption and the Ultraviolet Luminosity Density at $z \sim 3$ as Calibrated by Local Starburst Galaxies," *ApJ* **521**, 64–80 (Aug. 1999).
- [21] Stark, D. P., Ellis, R. S., Bunker, A., Bundy, K., Targett, T., Benson, A., and Lacy, M., "The Evolutionary History of Lyman Break Galaxies Between Redshift 4 and 6: Observing Successive Generations of Massive Galaxies in Formation," *ApJ* **697**, 1493–1511 (June 2009).
- [22] Bouwens, R. J., Illingworth, G. D., Oesch, P. A., Labbé, I., van Dokkum, P. G., Trenti, M., Franx, M., Smit, R., Gonzalez, V., and Magee, D., "UV-continuum Slopes of $> 4000 z \sim 4-8$ Galaxies from the HUDF/XDF, HUDF09, ERS, CANDELS-South, and CANDELS-North Fields," *ApJ* **793**, 115 (Oct. 2014).
- [23] Duncan, K., Conselice, C. J., Mortlock, A., Hartley, W. G., Guo, Y., Ferguson, H. C., Davé, R., Lu, Y., Ownsworth, J., Ashby, M. L. N., Dekel, A., Dickinson, M., Faber, S., Giavalisco, M., Grogin, N., Kocevski, D., Koekemoer, A., Somerville, R. S., and White, C. E., "The mass evolution of the first galaxies: stellar mass functions and star formation rates at $4 < z < 7$ in the CANDELS GOODS-South field," *MNRAS* **444**, 2960–2984 (Nov. 2014).
- [24] Salmon, B., Papovich, C., Finkelstein, S. L., Tilvi, V., Finlator, K., Behroozi, P., Dahlen, T., Davé, R., Dekel, A., Dickinson, M., Ferguson, H. C., Giavalisco, M., Long, J., Lu, Y., Reddy, N., Somerville, R. S., and Wechsler, R. H., "The Star-Formation Rate and Stellar Mass Relation of Galaxies at $3.5 \leq z \leq 6.5$ in CANDELS," *ArXiv e-prints* (July 2014).
- [25] Dickinson, M., Kartaltepe, J., Weiner, B., Kassin, S., Bournaud, F., Eisenhardt, P., Inami, H., and Pforr, J., "Are starbursts really mergers at high redshift? A kinematic investigation." NOAO Proposal (Aug. 2013).
- [26] Madau, P. and Dickinson, M., "Cosmic Star-Formation History," *ARA&A* **52**, 415–486 (Aug. 2014).
- [27] Balogh, M. L., Morris, S. L., Yee, H. K. C., Carlberg, R. G., and Ellingson, E., "Differential Galaxy Evolution in Cluster and Field Galaxies at $z \sim 0.3$," *ApJ* **527**, 54–79 (Dec. 1999).
- [28] Kauffmann, G., Heckman, T. M., White, S. D. M., Charlot, S., Tremonti, C., Brinchmann, J., Bruzual, G., Peng, E. W., Seibert, M., Bernardi, M., Blanton, M., Brinkmann, J., Castander, F., Csábai, I., Fukugita, M., Ivezić, Z., Munn, J. A., Nichol, R. C., Padmanabhan, N., Thakar, A. R., Weinberg, D. H., and York, D., "Stellar masses and star formation histories for 10^5 galaxies from the Sloan Digital Sky Survey," *MNRAS* **341**, 33–53 (May 2003).
- [29] Croton, D. J., Springel, V., White, S. D. M., De Lucia, G., Frenk, C. S., Gao, L., Jenkins, A., Kauffmann, G., Navarro, J. F., and Yoshida, N., "The many lives of active galactic nuclei: cooling flows, black holes and the luminosities and colours of galaxies," *MNRAS* **365**, 11–28 (Jan. 2006).
- [30] Fan, L., Lapi, A., De Zotti, G., and Danese, L., "The Dramatic Size Evolution of Elliptical Galaxies and the Quasar Feedback," *ApJ* **689**, L101–L104 (Dec. 2008).
- [31] Vestergaard, M. and Osmer, P. S., "Mass Functions of the Active Black Holes in Distant Quasars from the Large Bright Quasar Survey, the Bright Quasar Survey, and the Color-selected Sample of the SDSS Fall Equatorial Stripe," *ApJ* **699**, 800–816 (July 2009).
- [32] Krumholz, M. R., "The big problems in star formation: The star formation rate, stellar clustering, and the initial mass function," *Phys. Rep.* **539**, 49–134 (June 2014).
- [33] Elmegreen, B. G., "Star Formation Patterns and Hierarchies," in [*EAS Publications Series*], Charbonnel, C. and Montmerle, T., eds., *EAS Publications Series* **51**, 31–44 (Nov. 2011).
- [34] Adamo, A., Kruijssen, J. M. D., Bastian, N., Silva-Villa, E., and Ryon, J., "Probing the role of the galactic environment in the formation of stellar clusters, using M83 as a test bench," *MNRAS* **452**, 246–260 (Sept. 2015).
- [35] Johnson, K. E., Leroy, A. K., Indebetouw, R., Brogan, C. L., Whitmore, B. C., Hibbard, J., Sheth, K., and Evans, A. S., "The Physical Conditions in a Pre-super Star Cluster Molecular Cloud in the Antennae Galaxies," *ApJ* **806**, 35 (June 2015).
- [36] Kruijssen, J. M. D., "On the fraction of star formation occurring in bound stellar clusters," *MNRAS* **426**, 3008–3040 (Nov. 2012).
- [37] van Dokkum, P. G. and Conroy, C., "A substantial population of low-mass stars in luminous elliptical galaxies," *Nature* **468**, 940–942 (Dec. 2010).
- [38] Calzetti, D., Chandar, R., Lee, J. C., Elmegreen, B. G., Kennicutt, R. C., and Whitmore, B., "A Method for Measuring Variations in the Stellar Initial Mass Function," *ApJ* **719**, L158–L161 (Aug. 2010).
- [39] Cappellari, M., McDermid, R. M., Alatalo, K., Blitz, L., Bois, M., Bournaud, F., Bureau, M., Crocker, A. F., Davies, R. L., Davis, T. A., de Zeeuw, P. T., Duc, P.-A., Emsellem, E., Khochfar, S., Krajnović, D., Kuntschner, H., Lablanche, P.-Y., Morganti, R., Naab, T., Oosterloo, T., Sarzi, M., Scott, N., Serra, P., Weijmans, A.-M., and Young, L. M., "Systematic variation of the stellar initial mass function in early-type galaxies," *Nature* **484**, 485–488 (Apr. 2012).
- [40] Andrews, J. E., Calzetti, D., Chandar, R., Lee, J. C., Elmegreen, B. G., Kennicutt, R. C., Whitmore, B., Kissel, J. S., da Silva, R. L., Krumholz, M. R., O'Connell, R. W., Dopita, M. A., Frogel, J. A., and Kim, H., "An Initial Mass Function Study of the Dwarf Starburst Galaxy NGC 4214," *ApJ* **767**, 51 (Apr. 2013).

- [41] Whitmore, B. C., Chandar, R., and Fall, S. M., “Star Cluster Demographics. I. A General Framework and Application to the Antennae Galaxies,” *AJ* **133**, 1067–1084 (Mar. 2007).
- [42] Boutloukos, S. G. and Lamers, H. J. G. L. M., “Star cluster formation and disruption time-scales - I. An empirical determination of the disruption time of star clusters in four galaxies,” *MNRAS* **338**, 717–732 (Jan. 2003).
- [43] Jordán, A., McLaughlin, D. E., Côté, P., Ferrarese, L., Peng, E. W., Mei, S., Villegas, D., Merritt, D., Tonry, J. L., and West, M. J., “The ACS Virgo Cluster Survey. XII. The Luminosity Function of Globular Clusters in Early-Type Galaxies,” *ApJS* **171**, 101–145 (July 2007).
- [44] Chandar, R., Whitmore, B. C., Kim, H., Kaleida, C., Mutchler, M., Calzetti, D., Saha, A., O’Connell, R., Balick, B., Bond, H., Carollo, M., Disney, M., Dopita, M. A., Frogel, J. A., Hall, D., Holtzman, J. A., Kimble, R. A., McCarthy, P., Paresce, F., Silk, J., Trauger, J., Walker, A. R., Windhorst, R. A., and Young, E., “The Luminosity, Mass, and Age Distributions of Compact Star Clusters in M83 Based on Hubble Space Telescope/Wide Field Camera 3 Observations,” *ApJ* **719**, 966–978 (Aug. 2010).
- [45] Bastian, N., Konstantopoulos, I. S., Tranco, G., Weisz, D. R., Larsen, S. S., Fouesneau, M., Kaschinski, C. B., and Gieles, M., “Spectroscopic constraints on the form of the stellar cluster mass function,” *A&A* **541**, A25 (May 2012).
- [46] Calzetti, D., Kinney, A. L., and Storch-Bergmann, T., “Dust Obscuration in Starburst Galaxies from Near-Infrared Spectroscopy,” *ApJ* **458**, 132 (Feb. 1996).
- [47] Dale, J. E., “The modelling of feedback in star formation simulations,” *New A Rev.* **68**, 1–33 (Oct. 2015).
- [48] Cabrera-Ziri, I., Bastian, N., Davies, B., Magris, G., Bruzual, G., and Schweizer, F., “Constraining globular cluster formation through studies of young massive clusters - II. A single stellar population young massive cluster in NGC 34,” *MNRAS* **441**, 2754–2759 (July 2014).
- [49] Bianchi, L., Kang, Y., Hodge, P., Dalcanton, J., and Williams, B., “The role of ultraviolet imaging in studies of resolved and unresolved young stellar populations. M31 and M33,” *Advances in Space Research* **53**, 928–938 (Mar. 2014).
- [50] Bianchi, L., Kang, Y. B., Efremova, B., Thilker, D., Hodge, P., Massey, P., and Olsen, K., “Young stellar populations in the local group: an HST and GALEX comprehensive study,” *Ap&SS* **335**, 249–255 (Sept. 2011).
- [51] Bianchi, L., Efremova, B., Hodge, P., Massey, P., and Olsen, K. A. G., “A Treasury Study of Star-forming Regions in the Local Group. I. HST Photometry of Young Populations in Six Dwarf Galaxies,” *AJ* **143**, 74 (Mar. 2012).
- [52] Renzini, A. and Fusi Pecci, F., “Tests of evolutionary sequences using color-magnitude diagrams of globular clusters,” *ARA&A* **26**, 199–244 (1988).
- [53] Piotto, G., Milone, A. P., Bedin, L. R., Anderson, J., King, I. R., Marino, A., Nardiello, D., Aparicio, A., Barbuy, B., Bellini, A., Brown, T. M., Cassisi, S., Cunial, A., Dalessandro, E., D’Antona, F., Ferraro, F. R., Hidalgo, S., Lanzoni, B., Monelli, M., Ortolani, S., Renzini, A., Salaris, M., Sarajedini, A., van der Marel, R. P., Vesperini, E., and Zoccali, M., “The Hubble Space Telescope UV Legacy Survey of Galactic Globular Clusters. I. Overview of the Project and Detection of Multiple Stellar Populations,” *ArXiv e-prints* (Oct. 2014).
- [54] et al, B. N. *mnras* **436**, 2852 (2013).
- [55] Piotto, G., Milone, A. P., Bedin, L. R., Anderson, J., King, I. R., Marino, A. F., Nardiello, D., Aparicio, A., Barbuy, B., Bellini, A., Brown, T. M., Cassisi, S., Cool, A. M., Cunial, A., Dalessandro, E., D’Antona, F., Ferraro, F. R., Hidalgo, S., Lanzoni, B., Monelli, M., Ortolani, S., Renzini, A., Salaris, M., Sarajedini, A., van der Marel, R. P., Vesperini, E., and Zoccali, M., “The Hubble Space Telescope UV Legacy Survey of Galactic Globular Clusters. I. Overview of the Project and Detection of Multiple Stellar Populations,” *AJ* **149**, 91 (Mar. 2015).
- [56] Villanova, S., Piotto, G., and Gratton, R. G., “The helium content of globular clusters: light element abundance correlations and HB morphology. I. NGC 6752,” *A&A* **499**, 755–763 (June 2009).
- [57] Gratton, R., Sneden, C., and Carretta, E., “Abundance Variations Within Globular Clusters,” *ARA&A* **42**, 385–440 (Sept. 2004).
- [58] Decressin, T., Meynet, G., Charbonnel, C., Prantzos, N., and Ekström, S., “Fast rotating massive stars and the origin of the abundance patterns in galactic globular clusters,” *A&A* **464**, 1029–1044 (Mar. 2007).
- [59] D’Ercole, A., Vesperini, E., D’Antona, F., McMillan, S. L. W., and Recchi, S., “Formation and dynamical evolution of multiple stellar generations in globular clusters,” *MNRAS* **391**, 825–843 (Dec. 2008).
- [60] Bastian, N., Lamers, H. J. G. L. M., de Mink, S. E., Longmore, S. N., Goodwin, S. P., and Gieles, M., “Early disc accretion as the origin of abundance anomalies in globular clusters,” *MNRAS* **436**, 2398–2411 (Dec. 2013).
- [61] Vesperini, E., McMillan, S. L. W., D’Antona, F., and D’Ercole, A., “Dynamical evolution and spatial mixing of multiple population globular clusters,” *MNRAS* **429**, 1913–1921 (Mar. 2013).
- [62] Bellini, A., Anderson, J., van der Marel, R. P., Watkins, L. L., King, I. R., Bianchini, P., Chanamé, J., Chandar, R., Cool, A. M., Ferraro, F. R., Ford, H., and Massari, D., “Hubble Space Telescope Proper Motion (HSTPROMO) Catalogs of Galactic Globular Clusters. I. Sample Selection, Data Reduction, and NGC 7078 Results,” *ApJ* **797**, 115 (Dec. 2014).
- [63] Benz, W., Ida, S., Alibert, Y., Lin, D., and Mordasini, C., “Planet Population Synthesis,” *Protostars and Planets VI*, 691–713 (2014).

- [64] Alexander, R., Pascucci, I., Andrews, S., Armitage, P., and Cieza, L., “The Dispersal of Protoplanetary Disks,” *ArXiv e-prints* (Nov. 2013).
- [65] Hartmann, L., [*Accretion Processes in Star Formation*] (June 1998).
- [66] Hartmann, L., [*Accretion Processes in Star Formation: Second Edition*], Cambridge University Press (2009).
- [67] Gullbring, E., Hartmann, L., Briceño, C., and Calvet, N., “Disk Accretion Rates for T Tauri Stars,” *ApJ* **492**, 323–341 (Jan. 1998).
- [68] Herczeg, G. J. and Hillenbrand, L. A., “UV Excess Measures of Accretion onto Young Very Low Mass Stars and Brown Dwarfs,” *ApJ* **681**, 594–625 (July 2008).
- [69] Muzerolle, J., Calvet, N., and Hartmann, L., “Emission-Line Diagnostics of T Tauri Magnetospheric Accretion. II. Improved Model Tests and Insights into Accretion Physics,” *ApJ* **550**, 944–961 (Apr. 2001).
- [70] Valenti, J. A., Basri, G., and Johns, C. M., “T Tauri stars in blue,” *AJ* **106**, 2024–2050 (Nov. 1993).
- [71] Calvet, N. and Gullbring, E., “The Structure and Emission of the Accretion Shock in T Tauri Stars,” *ApJ* **509**, 802–818 (Dec. 1998).
- [72] Costigan, G., Scholz, A., Stelzer, B., Ray, T., Vink, J. S., and Mohanty, S., “LAMP: the long-term accretion monitoring programme of T Tauri stars in Chamaeleon I,” *MNRAS* **427**, 1344–1362 (Dec. 2012).
- [73] Manara, C. F., Beccari, G., Da Rio, N., De Marchi, G., Natta, A., Ricci, L., Robberto, M., and Testi, L., “Accurate determination of accretion and photospheric parameters in young stellar objects: The case of two candidate old disks in the Orion Nebula Cluster,” *A&A* **558**, A114 (Oct. 2013).
- [74] Manara, C. F. and Testi, L., “The imprint of accretion on the UV spectrum of young stellar objects: an X-Shooter view,” *Ap&SS* **354**, 35–39 (Nov. 2014).
- [75] Herczeg, G. J. and Hillenbrand, L. A., “An Optical Spectroscopic Study of T Tauri Stars. I. Photospheric Properties,” *ApJ* **786**, 97 (May 2014).
- [76] Rigliaco, E., Natta, A., Testi, L., Randich, S., Alcalá, J. M., Covino, E., and Stelzer, B., “X-shooter spectroscopy of young stellar objects. I. Mass accretion rates of low-mass T Tauri stars in σ Orionis,” *A&A* **548**, A56 (Dec. 2012).
- [77] Alcalá, J. M., Natta, A., Manara, C. F., Spezzi, L., Stelzer, B., Frasca, A., Biazzo, K., Covino, E., Randich, S., Rigliaco, E., Testi, L., Comerón, F., Cupani, G., and D’Elia, V., “X-shooter spectroscopy of young stellar objects. IV. Accretion in low-mass stars and substellar objects in Lupus,” *A&A* **561**, A2 (Jan. 2014).
- [78] Hartigan, P., Edwards, S., and Ghandour, L., “Disk Accretion and Mass Loss from Young Stars,” *ApJ* **452**, 736 (Oct. 1995).
- [79] Rigliaco, E., Pascucci, I., Gorti, U., Edwards, S., and Hollenbach, D., “Understanding the Origin of the [O I] Low-velocity Component from T Tauri Stars,” *ApJ* **772**, 60 (July 2013).
- [80] Natta, A., Testi, L., Alcalá, J. M., Rigliaco, E., Covino, E., Stelzer, B., and D’Elia, V., “X-shooter spectroscopy of young stellar objects. V. Slow winds in T Tauri stars,” *A&A* **569**, A5 (Sept. 2014).
- [81] De Marchi, G., Panagia, N., and Romaniello, M., “Photometric Determination of the Mass Accretion Rates of Pre-main-sequence Stars. I. Method and Application to the SN 1987A Field,” *ApJ* **715**, 1–17 (May 2010).
- [82] D’Antona, F. and Mazzitelli, I., “New pre-main-sequence tracks for M less than or equal to 2.5 solar mass as tests of opacities and convection model,” *ApJS* **90**, 467–500 (Jan. 1994).
- [83] Riess, A. G., Filippenko, A. V., Challis, P., Clocchiatti, A., Diercks, A., Garnavich, P. M., Gilliland, R. L., Hogan, C. J., Jha, S., Kirshner, R. P., Leibundgut, B., Phillips, M. M., Reiss, D., Schmidt, B. P., Schommer, R. A., Smith, R. C., Spyromilio, J., Stubbs, C., Suntzeff, N. B., and Tonry, J., “Observational Evidence from Supernovae for an Accelerating Universe and a Cosmological Constant,” *AJ* **116**, 1009–1038 (Sept. 1998).
- [84] Perlmutter, S., Aldering, G., Goldhaber, G., Knop, R. A., Nugent, P., Castro, P. G., Deustua, S., Fabbro, S., Goobar, A., Groom, D. E., Hook, I. M., Kim, A. G., Kim, M. Y., Lee, J. C., Nunes, N. J., Pain, R., Pennypacker, C. R., Quimby, R., Lidman, C., Ellis, R. S., Irwin, M., McMahon, R. G., Ruiz-Lapuente, P., Walton, N., Schaefer, B., Boyle, B. J., Filippenko, A. V., Matheson, T., Fruchter, A. S., Panagia, N., Newberg, H. J. M., Couch, W. J., and Project, T. S. C., “Measurements of Ω and Λ from 42 High-Redshift Supernovae,” *ApJ* **517**, 565–586 (June 1999).
- [85] Woosley, S. E. and Bloom, J. S., “The Supernova Gamma-Ray Burst Connection,” *ARA&A* **44**, 507–556 (Sept. 2006).
- [86] Rhoads, J. E., “How to Tell a Jet from a Balloon: A Proposed Test for Beaming in Gamma-Ray Bursts,” *ApJ* **487**, L1–L4 (Sept. 1997).